



Prepared in cooperation with St. Croix Watershed Research Station – Science Museum of Minnesota

Updates to the Madison Lake (Minnesota) CE-QUAL-W2 Water-Quality Model for Assessing Algal Community Dynamics

By Erik A. Smith and Richard L. Kiesling

Open-File Report 2019–XXXX

**U.S. Department of the Interior
U.S. Geological Survey**

U.S. Department of the Interior
DAVID BERNHARDT, Secretary

U.S. Geological Survey
James F. Reilly, Director

U.S. Geological Survey, Reston, Virginia: 2019

For more information on the USGS—the Federal source for science about the Earth, its natural and living resources, natural hazards, and the environment—visit [http://www.usgs.gov/](http://www.usgs.gov) or call 1-888-ASK-USGS (1-888-275-8747).

For an overview of USGS information products, including maps, imagery, and publications, visit <http://www.usgs.gov/pubprod/>.

Any use of trade, firm, or product names is for descriptive purposes only and does not imply endorsement by the U.S. Government.

Although this information product, for the most part, is in the public domain, it also may contain copyrighted materials as noted in the text. Permission to reproduce copyrighted items must be secured from the copyright owner.

Suggested citation:

Smith, E.A., and Kiesling, R.L., 2019, Updates to the Madison Lake (Minnesota) CE-QUAL-W2 water-quality model for assessing algal community dynamics: U.S. Geological Survey Open-File Report 2019-xxxx, xx p., <http://dx.doi.org/10.3133/XXXXX>.

ISSN XXXX-XXXX (online)

Acknowledgments

Funding for this study was provided by a grant from the Environmental and Natural Resource Trust Fund of Minnesota to the St. Croix Watershed Research Station – Science Museum of Minnesota. This report presents a compilation of information supplied by several agencies and individuals, mainly the Minnesota Department of Natural Resources and Minnesota Pollution Control Agency.

Annett Sullivan and Jeffrey Ziegeweid of the U.S. Geological Survey are greatly acknowledged for technical reviews of the report.

Contents

Acknowledgments.....	iii
Abstract	1
Introduction.....	2
Purpose and Scope	5
Study Area.....	5
Methods and Data.....	7
Water Balance.....	9
Hydraulic Boundary Conditions.....	9
Thermal Boundary Conditions.....	11
Meteorological Data	12
Water-Quality, Data Collection, Vertical Profiles, and Laboratory Analyses.....	13
Initial Conditions	15
Chemical Boundary Conditions	16
Model Parameters.....	16
Model Calibration and Validation	17
Water Balance.....	19
Temperature.....	20
Dissolved Oxygen	22
Algae.....	25
Macrophyte Growth.....	31
Nutrients	32
Model Limitations	38

Summary	41
References Cited	43

Figures

Figure 1. Map showing location of water-quality sampling sites for Madison Lake, Minnesota.....	6
Figure 2. Simulated and measured water temperature for vertical profiles at Madison Lake southwest deep point near Madison Lake, Minn. for eight dates in 2014, with values of mean absolute error (MAE) and root mean square error (RMSE).	21
Figure 3. Simulated and measured water temperature for vertical profiles at Madison Lake southwest deep point near Madison Lake, Minn. for nine dates in 2016, with values of mean absolute error (MAE) and root mean square error (RMSE).	21
Figure 4. Simulated and measured dissolved oxygen concentration for vertical profiles at Madison Lake southwest deep point near Madison Lake, Minn. for eight dates in 2014, with values of mean absolute error (MAE) and root mean square error (RMSE).	23
Figure 5. Simulated and measured dissolved oxygen concentration for vertical profiles at Madison Lake southwest deep point near Madison Lake, Minn. for nine dates in 2016, with values of mean absolute error (MAE) and root mean square error (RMSE).	23
Figure 6. Simulated and measured algal group distributions (diatoms, green algae, fixing cyanophyta, non-fixing (buoyant) cyanophyta, and flagellates) for the 1-meter depth at Madison Lake southwest deep point near Madison Lake, Minn., May 15 to November 1, 2014.	27
Figure 7. Simulated and measured chlorophyll <i>a</i> concentrations for the 1-meter depth at Madison Lake southwest deep point near Madison Lake, Minn. (segment 7) in Madison Lake, May 15 to November 1, 2014.....	29

Figure 8. Simulated and measured algal group distributions (diatoms, green algae, fixing cyanophyta, non-fixing (buoyant) cyanophyta, and flagellates) for the 1-meter depth at Madison Lake southwest deep point near Madison Lake, Minn., March 30 to November 23, 2016. 31

Figure 9. Simulated and measured chlorophyll a concentrations for the 1-meter depth at Madison Lake southwest deep point near Madison Lake, Minn. (segment 7) in Madison Lake, March 30 to November 23, 2016. 31

Figure 10. Simulated and measured dissolved ammonia concentrations at 1 meter below the water surface in model segment 7 containing the Madison Lake southwest deep point near Madison Lake, Minn., May 15 to November 1, 2014, with values of mean absolute error (MAE) and root mean square error (RMSE). 34

Figure 11. Simulated and measured dissolved ammonia concentrations at 1 meter below the water surface in model segment 7 containing the Madison Lake southwest deep point near Madison Lake, Minn., March 30 to November 23, 2016, with values of mean absolute error (MAE) and root mean square error (RMSE). 34

Figure 12. Simulated and measured dissolved nitrate plus nitrite concentrations at 1 meter below the water surface in model segment 7 containing the Madison Lake southwest deep point near Madison Lake, Minn., May 15 to November 1, 2014, with values of mean absolute error (MAE) and root mean square error (RMSE). 35

Figure 13. Simulated and measured dissolved nitrate plus nitrite concentrations at 1 meter below the water surface in model segment 7 containing the Madison Lake southwest deep point near Madison Lake, Minn., March 30 to November 23, 2016, with values of mean absolute error (MAE) and root mean square error (RMSE). 35

Figure 14. Simulated and measured dissolved orthophosphate concentrations at 1 meter below the water surface in model segment 7 containing the Madison Lake southwest deep point near Madison Lake, Minn., May 15 to November 1, 2014, with values of mean absolute error (MAE) and root mean square error (RMSE). 35

Figure 15. Simulated and measured dissolved orthophosphate concentrations at 1 meter below the water surface in model segment 7 containing the Madison Lake southwest deep point near Madison Lake, Minn., March 30 to November 23, 2016, with values of mean absolute error (MAE) and root mean square error (RMSE). 36

Figure 16. Simulated and measured total Kjeldahl nitrogen concentrations at 1 meter below the water surface in model segment 7 containing the Madison Lake southwest deep point near Madison Lake, Minn., May 15 to November 1, 2014, with values of mean absolute error (MAE) and root mean square error (RMSE)..... 37

Figure 17. Simulated and measured total Kjeldahl nitrogen concentrations at 1 meter below the water surface in model segment 7 containing the Madison Lake southwest deep point near Madison Lake, Minn., March 30 to November 23, 2016, with values of mean absolute error (MAE) and root mean square error (RMSE)..... 37

Figure 18. Simulated and measured total phosphorus concentrations at 1 meter and 16.5 meters below the water surface in model segment 7 containing the Madison Lake southwest deep point near Madison Lake, Minn., May 15 to November 1, 2014, with values of mean absolute error (MAE) and root mean square error (RMSE)..... 38

Figure 19. Simulated and measured total phosphorus concentrations at 1 meter and 15.5 meters below the water surface in model segment 7 containing the Madison Lake southwest deep point near Madison Lake, Minn., March 30 to November 23, 2016, with values of mean absolute error (MAE) and root mean square error (RMSE).38

Tables

Table 1. Location of continuous pressure transducers, water-quality sondes, thermistors, and discrete water-quality measurements used for the development of model input or calibration/validation of water temperature, dissolved oxygen, and water-quality constituents..... 6

Table 2. Water-quality methods for constituents analyzed in water samples from Madison Lake, 2014 and 2016. 14

Table 3. Relative counts and converted algal biomass (in milligrams per liter) for Madison Lake southwest deep point near Madison Lake, Minnesota, 2014 and 2016..... 14

Table 4. Initial constituent concentrations for the Madison Lake CE-QUAL-W2 model: 2014 calibration and 2016 validation runs..... 15

Table 5. Summary of mean absolute error (MAE) and root mean square error (RMSE) values for calibration (2014) and validation (2016) runs for Madison Lake at Madison Lake southwest deep point near Madison Lake, Minnesota (also known as southwest deep point).21

Conversion Factors

International System of Units to U.S. customary units

Multiply	By	To obtain
Length		
meter (m)	3.281	foot (ft)
meter (m)	39.37	inches (in.)
kilometer (km)	0.6215	mile (mi)
Area		
square kilometer (km ²)	0.3861	square mile (mi ²)
Volume		
cubic meter (m ³)	35.31	cubic foot (ft ³)
Flow rate		
meter per year (m/yr)	3.281	foot per year (ft/yr)
Energy		
watt per square meter (W/m ²)	0.3170	British thermal unit per hour per square foot (Btu/hr/ft ²)

Temperature in degrees Celsius (°C) may be converted to degrees Fahrenheit (°F) as °F = (1.8 × °C) + 32.

Vertical coordinate information is referenced to the North American Vertical Datum of 1988 (NAVD 88), unless otherwise indicated.

Horizontal coordinate information is referenced to the North American Datum of 1983 (NAD 83).

Elevation, as used in this report, refers to distance above the vertical datum.

Supplemental Information

Concentrations of chemical constituents in water are given in either milligrams per liter (mg/L) or micrograms per liter (µg/L).

Abbreviations

<	less than
DEM	digital elevation model
DHEL	Department of Health Environmental Laboratory
DO	dissolved oxygen
HAB	harmful algal bloom
MAE	mean absolute error
MNDNR	Minnesota Department of Natural Resources
NWIS	National Water Information System
R^2	coefficient of determination
RMSE	root mean square error
USACE	U.S. Army Corps of Engineers
USGS	U.S. Geological Survey
WSC	wind sheltering coefficient

Updates to the Madison Lake (Minnesota) CE-QUAL-W2 Water-Quality Model for Assessing Algal Community Dynamics

By Erik A. Smith and Richard L. Kiesling

Abstract

A previously developed CE-QUAL-W2 model for Madison Lake, Minnesota, simulated the algal community dynamics, water quality, and fish habitat suitability of Madison Lake under recent (2014) meteorological conditions. Additionally, this earlier model simulated the complex interplay between external nutrient loading, internal nutrient loading from sediment release of phosphorus, and the organic matter decomposition of the algal biomass. However, the partitioning of cyanobacteria within the modeling framework was simplified to one group and did not account for how different cyanobacteria populations are affected by light conditions, the usage of nitrogen, temperature growth ranges, and differences in settling rates. To get a better handle on the proliferation of cyanobacteria in Madison Lake, the model required updates to at least partition the cyanobacteria into a group that fixed nitrogen and a second, more buoyant cyanobacteria group, that did not independently fix nitrogen.

To address the shortcomings of simulating cyanobacteria in the earlier model, the U.S. Geological Survey (USGS), in cooperation with the St. Croix Watershed Research Station (Science Museum of Minnesota), updated the Madison Lake CE-QUAL-W2 model to better characterize cyanobacteria into two groups. In addition to updating the cyanobacteria group differentiation, the entire portion of the model that handles the simulation of algal community dynamics was updated while preserving the model's predictive capabilities for nutrients, water temperature, and dissolved oxygen. The calibration and validation of the model was done under recent meteorological conditions with large and persistent cyanobacteria blooms (2014 and 2016). Overall, the model simulations predicted the persistently large total phosphorus concentrations in Madison Lake's hypolimnion, key differences in nutrient concentrations between the two years, and cyanobacteria bloom persistence.

Introduction

Across the entire spectrum of freshwater lakes around the world, high anthropogenic nitrogen and phosphorus inputs into freshwater lakes have been implicated as one of the primary causes for the alarming rise in cyanobacteria blooms over the past several decades (Xu and others, 2010; Dolman and others, 2012; Paerl and Otten, 2013). These blooms can reduce the recreational and ecological value of lakes, including lakes across Minnesota. For Madison Lake, a fairly large and deep lake located in southern Minnesota, cyanobacteria have become an increasingly dominant component of the algal community. This creates a potential concern for the health of Madison Lake, as many cyanobacteria species can produce potent toxins and can lead to harmful algal blooms (HABs). When cyanobacteria form a toxic HAB, potential impairments include restricted recreational activities because of algal scums or algal mats and

the production of toxins (for example, microcystin) in amounts capable of threatening human health, domestic animals and wildlife (O'Neil and others, 2012; Graham and others, 2016). Exposure to environmental concentrations of cyanotoxins can cause hepatic, neurologic, respiratory, and dermatologic problems in humans (Merel and others, 2013; Loftin and others, 2016).

Although cyanobacteria (also known as cyanophyta) have been common components of the Madison Lake phytoplankton community for some time, recent Madison Lake data has shown a proliferation of cyanobacteria (Lindon and Heiskary, 2007; Lindon and Heiskary, 2009). From 2013 through 2018, routine field monitoring samples showed cyanobacteria as a fairly large percentage of the algal community, both by the overall number of individuals (counts) and the overall biovolume. Also, it was found that several cyanobacteria genera persisted throughout much of the summer and into the fall months (July through October).

The Minnesota Department of Natural Resources and other local resource managers are concerned that these cyanobacteria blooms could negatively impact Madison Lake. Madison Lake is a popular recreational lake for fishing, swimming, and boating and also has a dense community of year-round residents (Lindon and others, 2010). Persistent algal blooms, whether the blooms are cyanobacteria or other types of algae, can negatively impact the fishery indirectly by affecting dissolved oxygen. Madison Lake contains high-quality populations of fish species (Minnesota Department of Natural Resources, 2016) such as northern pike (*Esox lucius*), smallmouth bass (*Micropterus dolomieu*), bigmouth buffalo (*Ictiobus cyprinellus*), and bluegill sunfish (*Lepomis macrochirus*). Continuous monitoring of epilimnetic and hypolimnetic dissolved oxygen in Madison Lake has documented prolonged periods of hypoxia, associated with periods of long water residence time and sustained high levels of algal biomass that last for

weeks. When blooms enter stationary phase growth or start to senesce, bacteria mineralize the sinking algal biomass, consuming large amounts of oxygen, thereby decreasing dissolved oxygen concentrations. Large blooms can result in hypoxia areas, which, in turn, can endanger the fishery by creating habitat bottlenecks. So aside from the obvious concerns related to toxins, large algal blooms can have multiple negative effects on the overall health of Madison Lake.

Previous summaries of Madison Lake water quality have documented large inputs of nitrogen and phosphorus into Madison Lake (Lindon and others, 2018). A U.S. Geological Survey report (Smith and others, 2017) showed high levels of total phosphorus in the hypolimnion, in that case from 2014. The same report documented the development of a hydrodynamic and water-quality model for Madison Lake which suggested that a large component of the total phosphorus was due to internal loading from sediments during hypoxic or anoxic conditions. However, to get a handle on how a diverse algal community responds to shifts in external and internal loading of nutrients, particularly nitrogen and phosphorus, a sophisticated model that can simulate algal community dynamics is necessary. This earlier model, developed with the CE-QUAL-W2 modeling framework (Cole and Wells, 2015), did simulate the algal community into four different groups, including a general group for cyanobacteria (termed blue-green algae in the earlier report). However, this model's differentiation did not account for how different cyanobacteria populations are affected by light conditions, the usage of nitrogen, temperature growth ranges, and differences in settling rates.

To address the shortcomings of simulating cyanobacteria in the earlier model, the U.S. Geological Survey (USGS), in cooperation with the St. Croix Watershed Research Station (Science Museum of Minnesota) with support from the Minnesota Environment and Natural Resources Trust Fund (ENRTF), updated the Madison Lake CE-QUAL-W2 model. In addition

to updating the cyanobacteria group differentiation, the entire portion of the model that handles the simulation of algal community dynamics was updated while preserving the model's predictive capabilities for nutrients, water temperature, and dissolved oxygen. The calibration and validation of the model was done under recent meteorological conditions with large and persistent cyanobacteria blooms (2014 and 2016). With the completed model, further scenarios can be run as new Soil and Water Assessment Tool (SWAT) simulations become available that can provide external nutrient loading information for different management scenarios or past environmental conditions.

Purpose and Scope

The purpose of this report is to document updates to a previously developed CE-QUAL-W2 hydrodynamic and water-quality model of Madison Lake, Minnesota (Smith and others, 2017). The previous version simulated phytoplankton into four general algal communities or groups: (1) bacillariophyta and crysophyta (diatoms); (2) chlorophyta (green algae); (3) cyanophyta (blue-green algae); and, (4) haptophyta and cryptophyta (flagellates). For the updated model, the blue-green algae group, referred to as cyanophyta in this report, has been divided into two groups: a nitrogen-fixing cyanophyta group, generally representative of *Anabaena*, *Dolichospermum*, and *Cylindrospermopsis*, and a non-fixing, buoyant cyanophyta group, generally representative of *Planktothrix*, *Microcystis*, and *Woronichinia*.

Study Area

Madison Lake (fig. 1) in Blue Earth County, Minnesota, is in the Le Sueur River Basin, part of the greater Minnesota River Basin (Lindon and others, 2010). Madison Lake is weakly dimictic, generally starting off as well-mixed before early summer, with a weak thermocline that

develops in the summer months; the lake mixes again in the late fall (Lindon and others, 2010). Dissolved oxygen is well-mixed in the early spring (April to May) and late fall (mid-October), with a substantial portion of the hypolimnion becoming anoxic by mid-summer; however, anoxia can develop earlier in some years and subsist late into the fall, especially when the lake's thermocline develops early (Lindon and others, 2010). The water balance of the drainage basin for Madison Lake is typically controlled by a spring snowmelt in late March or early April, followed by periodic large rain events in the summer. The mean precipitation in the region for 1981–2010 is 0.82 meter per year (m/yr) (National Centers for Environmental Information, 2016).

Figure 1. Map showing location of water-quality sampling sites for Madison Lake, Minnesota.

Table 1. Location of continuous pressure transducers, water-quality sondes, thermistors, and discrete water-quality measurements used for the development of model input or calibration/validation of water temperature, dissolved oxygen, and water-quality constituents.

Primary inflows to Madison Lake are in the northeast and southeast parts of the lake, both primary sampling locations for nutrient and major inorganic constituents, water temperature, and streamflow (table 1). The unnamed stream to Madison Lake at CR-48 near Madison Lake, Minn. (USGS station number 05320130 [U.S. Geological Survey, 2019a]; hereafter referred to as the “northeast inlet”) flows into the relatively large and shallow northeast bay of Madison Lake. The unnamed stream between Schoolhouse and Goolsby Lakes southeast of Madison Lake, Minn. (USGS station number 05320140; hereafter referred to as the “southeast inlet”) flows into the shallow part of the smallest bay (by area) along the southeast shoreline. The main primary outflow for Madison Lake is the site Madison Lake outlet to Mud Lake South of Madison Lake,

Minn. (USGS station number 05320170 [U.S. Geological Survey, 2019a]; hereafter referred to as the “Madison Lake outlet”), located along the southwest part of the lake.

The lake has three distinct bays, with two of the three bays containing deep areas. The deep area in the southwest bay, also the largest deep area by areal extent, was sampled at site Madison Lake southwest deep point near Madison Lake, Minn. (hereafter referred to as “southwest deep point”) with a depth of approximately 18 m. This location was used for extensive in-lake water-quality sampling, periodic vertical profiles of water temperature and DO, and continuous monitoring of water temperature at various depths.

Methods and Data

The Madison Lake CE-QUAL-W2 model was previously developed for 2014 to simulate algal community dynamics, water-surface elevations, flow, water quality, and fish habitat suitability (Smith and others, 2017). This study updated the original model to re-distribute the algal community into five distinct algal groups or divisions rather than four groups, re-calibrating the updated model for 2014 and validating the model for 2016. Both the original and updated versions were developed with CE-QUAL-W2 (version 4.0, available at <http://www.ce.pdx.edu/w2/>), a two-dimensional, laterally averaged, hydrodynamic and water-quality model originally developed by the USACE and currently supported by Portland State University (Cole and Wells, 2015). The CE-QUAL-W2 model calculates the hydrodynamic properties of water-surface elevation, velocities, and temperature and can simulate water-quality variables in addition to temperature. An advantage of the CE-QUAL-W2 model is that the hydrodynamic and water-quality modules are coupled together through an equation of state for density, dependent on temperature, suspended solids, and dissolved solids. This enables the

water-quality model to feed back into the hydrodynamic part of the model; however, because of this coupling, changes to the model specifications for algal growth and senescence can affect the other parts of the model. Therefore, the changes to the algal dynamics and some other updates required a reassessment of the entire model fit.

The CE-QUAL-W2 computational grid, based on available bathymetric data (Minnesota Geospatial Information Office, 2016) and a digital elevation model (DEM) (U.S. Geological Survey, 2016), was left unaltered and is described in detail in Smith and others (2017). In summary, the CE-QUAL-W2 grid was separated into segments that laterally average across the lake, with individual segments grouped together into branches. Each branch is grouped together to represent the entire computational grid of the water body. For Madison Lake, the CE-QUAL-W2 water body (fig. 1) was grouped together from two separate branches: (1) branch 1 starts at segment 2 and continues through segment 9; (2) branch 2 separates out the southeast part of Madison Lake, where the southeast inlet flows into the lake, and connects to branch 1 at segment 9 via segment 15.

This project followed a similar calibration strategy as other CE-QUAL-W2 modeling projects completed by the Upper Midwest Water Science Center Integrated Ecosystems Systems team (Smith and others, 2014; Smith and others, 2017; Smith and others, 2018). Calibration targets included a water balance calibration based on water-surface elevation, chlorophyll *a*, algae, and nutrients (ammonia, nitrate plus nitrite, total Kjeldahl nitrogen, total phosphorus, orthophosphate). As vertical variations in temperature and dissolved oxygen are important for distinguishing temporal variations in the lake epilimnion, hypolimnion, and mixed layers, emphasis was considered for the synoptic depth profiles of temperature and dissolved oxygen from the southwest deep point.

The CE-QUAL-W2 model required time series inputs of hydrological, thermal, water quality, and meteorological data. A summary of the discrete and continuous data collected for Madison Lake, further split by sampling locations, is shown in table 1. All the input data used for calendar year 2014 was documented in Smith and others (2017). The same basic data and sources was used for 2016, with the exception that continuous streamflow and temperature was unavailable for 2016, so a surrogate dataset was required and discussed further in the “Hydraulic and Thermal Boundary Conditions”.

Water Balance

The water balance of Madison Lake for May 15–November 1, 2014 was left unaltered (Smith and others, 2017), with a new water balance required for March 30–November 23, 2016. Similar to the 2014 water balance, the 2016 water balance was completed by comparing measured water levels to simulated water levels. However, unlike 2014, continuous water levels were unavailable for the Madison Lake outlet (USGS station number 05320170). Instead, the simulated water levels were compared to the daily water-surface elevations collected by the Lake Level Minnesota Monitoring Program (Minnesota Department of Natural Resources, 2019a) and available from the Minnesota Department of Natural Resources (MNDNR) Lake Finder website (Minnesota Department of Natural Resources, 2019b).

Hydraulic Boundary Conditions

Lake inflow used in the CE-QUAL-W2 model were obtained from two separate channels that flow into Madison Lake. The northeast inlet streamflow (fig. 1; table 1) was measured in the channel connecting several small lakes and wetlands to Madison Lake. The southeast inlet streamflow (fig. 1; table 1) was measured in the channel connecting Schoolhouse and Goolsby

Lake to Madison Lake. Submersible pressure transducers were installed for the northeast inlet, southeast inlet, and Madison Lake outflow from May–November 2014. These transducers collected continuous water-surface level (stage or gage height) measurements every 15 minutes. Three corresponding measurements of streamflow and water-surface level measurements were made at each inflow site in 2014 (U.S. Geological Survey, 2019) by the MNDNR to construct an elevation-streamflow rating table, as discussed in Smith and others (2017) and presented in appendix table 1–1 of the same report. In summary, the elevation-streamflow rating curves were developed using graphical plotting methods similar to those described in Rantz and others (1982a, 1982b), with linear extrapolations added to the upper and lower end of the rating curves to estimate streamflows outside of the range of measured streamflows. The Madison Lake outflow, located along the southwest part of the lake, was also estimated through an elevation-streamflow rating curve, based upon four direct measurements made in 2014.

For 2016, no continuous water level measurements were available for either of the two inflow sites or the lake outflow. However, the model still requires streamflow input into the model, ideally sub-daily measurements. Without such a record available, the 2014 elevation-streamflow rating table was applied to the daily water-surface elevations from the Lake Level Minnesota Monitoring Program (Minnesota Department of Natural Resources, 2019a; 2019b). By using this methodology, daily inflows and outflow were calculated and input into the model. The daily water-surface elevations used for 2016, available from the Lake Finder website, are also available as part of the full CE-QUAL-W2 model archive (Smith, 2019) in the `el_obs.csv` file (in meters) available on USGS ScienceBase.

For both 2014 and 2016, additional water inflows to Madison Lake were assumed from un-gaged locations in the lake and from groundwater flow, known as distributed tributary flow.

This distributed tributary flow was input into the model in daily time steps and distributed evenly across all the model segments. To account for this additional flow, water was iteratively added to the distributed tributary flow (also known as QDT) through successive model runs until a satisfactory match was attained between simulated and measured water-surface elevations.

Thermal Boundary Conditions

Inflowing water temperature was collected in 2014 by the same submersible pressure transducers for water levels: the northeast inlet and the southeast inlet. The temperatures were then converted to the appropriate data format for CE-QUAL-W2 and applied as `tin_br1`, the inflowing water temperature via the northeast inlet into branch 1, and `tin_br2`, the inflowing water temperature via the southeast inlet into branch 2 (Smith and others, 2017; Smith, 2019). The distributed tributary flow also had associated temperature records within the model framework, applied as `tdt_br1` and `tdt_br2` for the two separate branches. In both cases, a continuous temperature record from a nearby observation well with a depth of 3.8 meters (Minnesota Unique Identification Number 792526) was assumed as the distributed tributary flow temperature. No conversion was done with this temperature record and is available as part of the CE-QUAL-W2 archive (Smith, 2019). As this continuous record was available from 2013 through 2018, both 2014 and 2016 had a full record available. The daily mean temperatures for the northeast inlet (USGS station number 05320130) and for the southeast inlet (USGS station number 05320140) are available online through NWIS (U.S. Geological Survey, 2019); additionally, the ScienceBase archive for the CE-QUAL-W2 model (Smith, 2019) includes the 2014 inflow water temperatures.

However, as with the flow data, no direct water temperatures were available for 2016 for either the northeast or southeast inlet. Instead, a surrogate water temperature dataset had to be

constructed. Using a relationship between water temperature and air temperature, similar to a technique applied to central United States streams by Preud'homme and Stefan (1992), a regression between the daily air temperature (available from the Mankato Regional Airport) and the daily water temperatures from the two inlet transducers was applied. For branch 1, the following mathematical relation between daily air temperature and daily water temperature (eqn. 1), based on 2014 data, was applied to 2016 daily air temperatures to create a surrogate branch 1 temperature record with a coefficient of determination (R^2) of 0.87:

$$\text{Temperature (Branch 1)} = 1.0208 * \text{Daily Air Temperature} - 1.4595, R^2 = 0.87 \quad (1)$$

For branch 2, the following mathematical relation between daily air temperature and daily water temperature (eqn. 2), also based on 2014 data, was applied to 2016 daily air temperatures to create a surrogate branch 2 temperature record with a R^2 of 0.90:

$$\text{Temperature (Branch 2)} = 0.993 * \text{Daily Air Temperature} + 0.4015, R^2 = 0.90 \quad (2)$$

As with the 2014 temperature data, the ScienceBase archive (Smith, 2019) includes the 2016 inflow and distributed tributary water temperatures.

Meteorological Data

Meteorological data are required as input to the CE-QUAL-W2 model because of the importance of surface boundary conditions to the overall behavior of the model, specifically surface heat exchange, solar radiation absorption, wind stress, and gas exchange. Required meteorological data include air temperature, dew point temperature, wind speed, wind direction, and cloud cover. All unit conversions from the meteorological data to the required units for the model were straightforward with the exception of cloud cover. The qualitative sky cover parameter (that is, clear, scattered, broken, and overcast) was converted to an integer value ranging from 0 to 10: clear is 1, scattered (1/8 to 1/2 cloud coverage) is 5, and overcast is 10. All

of the required data were available at hourly intervals for the Mankato Regional Airport (U.S. Air Force station identification number 726585) from the Climate Data Online portal (National Climatic Data Center, 2016; National Climatic Data Center, 2018), located <12.5 kilometers (km) west of Madison Lake. Based on the latitude and longitude of the lake and the required meteorological inputs, evapotranspiration was included in the water balance as an internal CE-QUAL-W2 calculation.

Water-Quality, Data Collection, Vertical Profiles, and Laboratory Analyses

Limnological characteristics, including properties that could affect trophic state, were examined at the southwest deep point. This site was sampled by MNDNR staff five times in 2014 (Smith and others, 2017) and between 5-11 times, depending on the constituent, for 2016. Samples were collected near the surface (between 0 and 2 meters) and at depth, averaging between 15.5 and 16.5 meters, using a Kemmerer sampler (Wildco 1200E; Wildlife Supply Co., Yulee, Florida) and were analyzed using the methods in table 2 to determine concentrations of nutrients, chlorophyll *a*, total dissolved solids, major ions (total silica and dissolved iron), and algal counts. Water samples were filtered (through a 0.45-micrometer filter for dissolved analysis or not filtered for total analysis) and preserved as required (U.S. Environmental Protection Agency, 1993a, 1993b, 1993c, 1994d). Alkalinity was determined by incremental titration at the field location (Wilde, 2006). Secchi-disk transparency (Wetzel, 2001) was measured at each vertical profile location to estimate photic depth. Vertical profiles (approximately 1-m intervals) of temperature, DO concentration, pH, and specific conductance were measured by MNDNR staff with a multiparameter Hydrolab sonde at each lake site in conjunction with the water samples.

Table 2. Water-quality methods for constituents analyzed in water samples from Madison Lake, 2014 and 2016.

Sampling also was done by the MNDNR at the inflows for both lakes (table 1). The same constituents and methodologies as the limnological sites were followed for these inflow sites. Sampling frequency for the inflow sites varied between the two inlets and two years, sampled 4-5 times in 2014 and 5-6 times in 2016. Water samples collected by the MNDNR at the lake, inflow, and outflow sites were analyzed by the Minnesota Department of Health Environmental Laboratory (DHEL) in St. Paul, Minn., except for the algae data. All the samples analyzed by the Minnesota DHEL have been previously reviewed and published and are available online (Minnesota Pollution Control Agency, 2018). The algae data were produced by a phytoplankton enumeration technique performed by PhycoTech, Inc. (PhycoTech, 2019); all of the raw algal data are presented in table 3, presented by relative count, and then converted to algal biomass by assuming an algal biomass (in milligrams per liter) to chlorophyll *a* (in micrograms per liter) ratio of 0.05 and multiplying by the chlorophyll *a* concentration collected on the same day. This ratio is different than the ratio applied for Smith and others (2017) for 2014 data, so table 3 supersedes the Smith and others (2017) unless applied with the earlier version of the model.

Table 3. Relative counts and converted algal biomass (in milligrams per liter) for Madison Lake southwest deep point near Madison Lake, Minnesota, 2014 and 2016.

A primary data-quality objective was to ensure that samples were representative of the water bodies under investigation. Quality assurance was assessed with specific procedures, such as instrument calibration, to ensure data reliability and assess the quality of the sample data. The quality-assurance plan for this study followed MNDNR guidelines (Anderson and Martin, 2015).

Additional quality assurance specific to Minnesota DHEL is available online (Minnesota Department of Health, 2016). Results from available quality-assurance data associated with water-quality data used for input to the model and for calibration and validation of the model were reviewed prior to the modeling efforts. Overall, the water-quality datasets (discrete samples collected at specific streamflow or lake elevations) for the calibration and validation periods were considered appropriate for the range of environmental conditions simulated for this study.

Initial Conditions

Water-quality modeling was incorporated into the lake hydrodynamic model. Each simulated constituent (including temperature) must have an initial, single concentration for the entire lake or a gridwide initial vertical profile of concentrations at the start of each model run. Initial constituent concentrations are presented in table 4 for the calibration (2014) run and the validation (2016) run; initial constituent concentrations were considered uniform throughout both lakes for every segment and layer, except in cases with a reported range of values in a vertical profile. It should be noted that differences exist between the starting initial constituent concentrations for the algal concentrations from the original Madison Lake CE-QUAL-W2 model (Smith and others, 2017) and the updated CE-QUAL-W2 model presented in this report (table 2). In addition to water quality constituents, an initial water-surface elevation and water temperature were also set to the measured value at the simulation start for both lakes.

Table 4. Initial constituent concentrations for the Madison Lake CE-QUAL-W2 model: 2014 calibration and 2016 validation runs.

Chemical Boundary Conditions

Each simulated water-quality constituent, including total dissolved solids, nutrients, silica, iron, organic matter, and inorganic carbon, must have a daily concentration value for all inflow tributaries (including distributed tributary flow). Because of the low frequency of discrete water-quality samples, a mean daily concentration value was linearly interpolated between the discrete samples for each inflow tributary or a single concentration was applied for the entire model run for each inflow tributary. The distributed tributary inflow constituents were based on the mean concentrations for the northeast inlet site for branch 1 and the southeast inlet for branch 2.

Organic matter concentrations were back-calculated from the total Kjeldahl nitrogen concentration minus the dissolved ammonia concentration, with an additional calculation based on a linear relation between streamflow and the particulate organic nitrogen to total organic nitrogen ratio (Smith and others, 2014). Organic matter concentrations were then further divided into four separate pools, as required by the CE-QUAL-W2 model (Cole and Wells, 2015): labile dissolved, refractory dissolved, labile particulate, and refractory particulate, with dissolved and particulate pools separated into labile and refractory at 30 and 70 percent, respectively.

Model Parameters

Numerous CE-QUAL-W2 models have shown that the default hydraulic parameters are robust across different hydrologic settings (Cole and Wells, 2015). Most of the default hydraulic parameters that control the hydrodynamics and heat exchange provided within CE-QUAL-W2 or the CE-QUAL-W2 manual (Cole and Wells, 2015). The density control for all inflows in the

model allowed for the water inflows to match up with the layers within the lake that corresponded to the inflow density.

For the water-quality algorithms, over 200 parameters control the constituent kinetics. An advantage of CE-QUAL-W2 is the modular design that allows for control of the water-quality constituents by adding specific subroutines. Many of these parameters were optional depending on the inclusion of groups such as epiphyton, zooplankton, macrophytes, and algae. As with the hydraulic and heat exchange parameters that control the hydrodynamics, all the parameters were time and space invariant. The option exists to vary some parameters, such as the extinction coefficient of water; however, not enough data were collected to justify dynamic control of any parameters. All the parameterization for the updated Madison Lake CE-QUAL-W2 is available through the CE-QUAL-W2 control file, available in the ScienceBase archive (Smith, 2019). Many of the parameters were left as the default values, whereas the remaining parameters were adjusted during the calibration process. Guidance for adjusting selected parameters also came from other USGS CE-QUAL-W2 model applications (Bales and Robbins, 1999; Flowers and others, 2001; Green and others, 2003; Sullivan and Rounds, 2004; Galloway and Green, 2006; Galloway and others, 2008; Sullivan and others, 2011; Smith and others, 2014; Cole and Wells, 2015).

Model Calibration and Validation

The degree of fit between the simulated results and measured lake values was considered during model calibration. The two values utilized to evaluate the degree of fit were the MAE and the RMSE. The MAE, computed by equation 3 (for example, see usage in Smith and others,

2017 and Smith and others, 2018), is a measure of the mean difference between the simulated (model) value and the measured value:

$$MAE = \frac{1}{n} \sum_{i=1}^n |simulated\ value - measured\ value| \quad (3)$$

where

n is the number of observations.

For example, an MAE of 1.0 milligram per liter (mg/L) for DO means that the simulated value is on average within 1.0 mg/L of the measured DO value. The RMSE is a slightly different metric in that it indicates the amount of deviation between the simulated value and the measured value. The RMSE, as computed by equation 4 (for example, see usage in Smith and others, 2014), gives the deviation between the simulated value and the measured value approximately 67 percent of the time:

$$RMSE = \sqrt{\frac{1}{n} \sum_{i=1}^n (simulated\ value - measured\ value)^2} \quad (4)$$

where

n is the number of observations.

The degree of fit between the simulated and measured outlet water-surface elevation was only considered during the initial water balance calibration for each year. The early focus on the water balance made certain that the amount of flow in and out of the lake is properly considered before the subsequent water temperature, DO, algae, and nutrients followed, using the MAE and RMSE metrics.

Refined calibration focused on the vertical profiles of temperature and DO (fig. 1; table 1). Additionally, the refined calibration step included the water-quality parameters highlighted previously (ammonia, nitrate plus nitrite, total Kjeldahl nitrogen, total phosphorus,

orthophosphate, and chlorophyll *a*). Final refinement of model parameters was achieved with the realization of low MAE and RMSE values for most of the target constituents. Values of MAE and RMSE below 1 degree Celsius (°C) and <1 mg/L for DO were ideal but not possible for every profile. The MAE and RMSE values for other water-quality parameters were operationally defined by other USGS reports utilizing CE-QUAL-W2, such as Smith and others (2014), which included Lake Carlos, Elk Lake, and Trout Lake and Smith and others (2017), which included the original Madison Lake model and Pearl Lake, another Sentinel Lake. Most model runs included one adjustment with a subsequent model run to characterize the parameter sensitivity.

Water Balance

Before the water temperature and water-quality calibration could proceed, the differences between the simulated and measured water-surface elevations were rectified for 2016, as the 2014 water balance was completed during the initial model calibration (Smith and others, 2017). Similar to the calibration strategy for 2014 (Smith and others, 2017), the initial attempt to achieve a water balance for Madison Lake used the two gaged tributaries, the northeast inlet and southeast inlet (table 1), as the sole inflows for the calibration period of March 30–November 23, 2016; however, the simulated water-surface elevation was below the measured water-surface elevation, which indicated that additional water sources to the lake existed, such as ungaged tributaries and groundwater.

Two different distributed tributary flows were added iteratively for each of the two water bodies of Madison Lake to include unaccounted inflow. In addition to unaccounted inflows and groundwater flow, the 2016 water balance included a higher percentage of distributed tributary flow compared to the ratio of branch inflows to distributed tributary flow in 2014. For 2014, approximately 15 percent of the total flow during the calibration period (May 15–November 1,

2014) was from the distributed tributary flow. Alternatively, approximately 51 percent of the total flow during the validation period (March 30–November 23, 2016) was from the distributed tributary flow. A comparison between daily flows calculated directly from the transducer water levels to daily flows calculated from the 2014 Lake Level Minnesota Monitoring Program yielded an R^2 of 0.98 and 0.97, respectively, for branch 1 inflow and branch 2 inflow, demonstrating that using the lake water-surface elevation rather than transducer water levels was an appropriate technique for 2016. However, the lack of sub-daily resolution combined with the possibility of bias from using the lake water-surface elevation led to the higher percentage of distributed tributary flow for 2016. The water balance was still rectified for 2016, with MAE and RMSE values of <0.03 m for the simulated water-surface elevations.

Temperature

The simulated water temperature results from both the calibration (2014) and validation (2016) were compared to vertical profiles of lake water temperatures at the southwest deep point site, generally collected during MNDNR water-quality sampling trips. Comparisons to the same 2014 profiles were made for the original Madison Lake model calibration (Smith and others, 2017), but new comparisons were warranted to make sure that the updated model still adequately captured the lake's temperature dynamics.

A total of eight dates from 2014 are shown in figure 2, and nine dates from 2016 are shown in figure 3. For 2014, the model consistently attained MAE and RMSE values <1.0 °C for all eight dates, with several values <0.5 °C. The temperature calibration did not differ much from the original Madison Lake model. For the combined vertical profiles, the MAE and RMSE values were 0.55 and 0.70 °C, respectively (table 5), compared to the original Madison Lake model with 0.53 and 0.68 °C, respectively, so almost identical between the original calibration

and the updated model. As with the original model, the location and slope of the simulated thermocline matched the measured thermocline. For 2016, the model also consistently attained MAE and RMSE values <1.0 °C for eight of nine dates, with one exception early in the year slightly simulated too warm. For the combined 2016 vertical profiles, the MAE and RMSE values were 0.67 and 0.81 °C, respectively (table 5).

Figure 2. Simulated and measured water temperature for vertical profiles at Madison Lake southwest deep point near Madison Lake, Minn. for eight dates in 2014, with values of mean absolute error (MAE) and root mean square error (RMSE).

Figure 3. Simulated and measured water temperature for vertical profiles at Madison Lake southwest deep point near Madison Lake, Minn. for nine dates in 2016, with values of mean absolute error (MAE) and root mean square error (RMSE).

Table 5. Summary of mean absolute error (MAE) and root mean square error (RMSE) values for calibration (2014) and validation (2016) runs for Madison Lake at Madison Lake southwest deep point near Madison Lake, Minnesota (also known as southwest deep point).

The influential boundary conditions that affect water temperature included sediment temperature, initial lake water temperature, and inflow water temperature. The temperature substitution for 2016, using air temperatures to simulate water temperatures, did not seem to have a large effect on the 2016 model validation given the low MAE and RMSE values. Meteorological effects include air temperature, wind velocity, wind direction, and solar radiation. Wind sheltering effects, as augmented through the wind sheltering coefficient (WSC) file, were still important for the 2016 validation. The WSC input file considers boundary effects on wind mixing, such as topography and shoreline tree cover, with a range from 50 to 72 percent

of the full wind value for 2016 and 50 to 64 percent for 2014, except for a value of 100 percent at the beginning of both years. Several hydraulic and thermal parameters also affect water temperature. Most of these parameters were left identical to the original Madison Lake model, with the exception of an increase from 1.5 to 2.0 for the CBHE coefficient that controls sediment heat exchange and a slight increase in the sediment temperature by 0.3 °C. One other set of critical parameters altered for the updated model were the short wave solar radiation extinction coefficients due to various algal groups (EXA1, EXA2, EXA3, EXA4, EXA5), which were all adjusted from 0.1 to 0.2 for each group, the recommended default CE-QUAL-W2 value (Cole and Wells, 2015; Smith, 2019).

Dissolved Oxygen

Accurately simulating DO is critical in determining the size of summer habitat refugia for important game fish species because their thermal requirements often confine them below the epilimnion where they are vulnerable to mass die offs because of a lack of DO. Even cool-water and warm-water fish species have upper thermal tolerances. If these fish subsist for long periods in warmer waters in combination with low DO levels, even noncold-water fish can be subject to die offs (Fang and others, 1999) based on oxythermal constraints.

Within the CE-QUAL-W2 model, many sources and sinks are available for DO, which makes DO likely the most complicated constituent to model. Sources include inflows, atmospheric exchange across the lake surface, and algal photosynthesis (Cole and Wells, 2015). Sinks include decay mechanisms such as bacterial respiration of dissolved and solid-phase organic matter (labile and refractory) in the water column and lake sediment. Other simulated sinks include algal respiration, macrophyte respiration, ammonia and nitrite nitrification, and

exchange back to the atmosphere and into sediments (Cole and Wells, 2015). The values used for these parameters are part of the CE-QUAL-W2 control file (Smith, 2019).

With varying success, the model captured the trajectories of DO concentrations at multiple depths over time, which indicated that the model was accurately simulating the underlying metabolic processes in each lake. For the DO calibration (2014) and validation (2016), the principal calibration targets were the lake profile data from the southwest deep point site, available from monthly vertical DO profiles collected by MNDNR personnel during water-quality sampling trips. Generally, DO measurements were recorded for each meter below water surface. Simulated and measured DO concentrations are shown for a total of eight dates for 2014 (fig. 4), and a total of nine dates for 2016 (fig. 5). Overall, the simulated DO concentrations tracked the measured concentrations from the southwest deep point site.

Figure 4. Simulated and measured dissolved oxygen concentration for vertical profiles at Madison Lake southwest deep point near Madison Lake, Minn. for eight dates in 2014, with values of mean absolute error (MAE) and root mean square error (RMSE).

Figure 5. Simulated and measured dissolved oxygen concentration for vertical profiles at Madison Lake southwest deep point near Madison Lake, Minn. for nine dates in 2016, with values of mean absolute error (MAE) and root mean square error (RMSE).

Similar to water temperature, the same 2014 DO profiles were compared for the original Madison Lake model calibration (Smith and others, 2017), but new comparisons were warranted to make sure that the updated model still adequately captured the lake's DO dynamics. Generally, where the greatest change in DO occurred, the simulated concentrations matched the depth and slope of the measured concentrations. Also, compared to the earlier model

comparisons, the same observations and conclusions from Smith and others (2017) can be made for the updated model calibration (2014). For example, the maximum midwater DO maximum between 3 and 6 m on May 29, 2014, showed little difference between the simulated and measured values as reflected with the low MAE and RMSE values (<0.6 mg/L). Also similar to the original calibration, the minimal hypolimnion oxygen levels starting from around June 3, 2014, were maintained until sometime between the August 26 and September 17 DO profiles. By September 17, the lake began to overturn, as shown for DO (fig. 4) and lake water temperature (fig. 2). The simulated DO concentrations for September 17 were greater at depth, so the lake overturn started to occur 7 to 10 days earlier in the model than the measured lake values. For the combined vertical DO profiles, the MAE and RMSE values were 0.86 and 1.22 mg/L, respectively (table 5), compared to the original Madison Lake model with 0.68 and 1.15 mg/L, respectively,

For the 2016 validation, the simulated DO still captured the DO trajectories, but did not attain as low MAE and RMSE values; for the combined 2016 vertical profiles, the MAE and RMSE values were 0.91 and 1.46 mg/L, respectively. However, despite these higher values, the model simulated the general DO trajectories throughout the year from May to September with the nine profiles. The largest discrepancy between the measured and simulated results was the lack of simulated DO supersaturation in the shallower mixed layer. This discrepancy could be caused by the lack of simulated algal growth earlier in the year, such that an earlier algal bloom missed or not captured with the model would have caused larger simulated DO values in the shallow mixed layer. Alternatively, the model did an adequate simulation of the hypolimnetic oxygen minimums, both with depth and timing. Overall, the 2016 model validation did show that

the model could capture DO dynamics for two years with different algal community dynamics and a different total algal biomass.

As far as parameter changes with the updated model, significant changes were made to the algal community dynamics, as discussed in the “Algae” section. Since algal dynamics played a large part in controlling the DO dynamics, those changes that could have affected DO are discussed separately. However, other major parameters that can control limnological DO concentrations, such as the decay rates of different organic matter pools, were unaltered from the original Madison Lake model. Also, the sediment oxygen demand (parameter SOD) was unaltered from the original Madison Lake model (2.5 mg/L). The equation for calculating reaeration was changed from equation #9 to equation #3, upon a determination that equation #3 is more appropriate for water bodies with lower flow-through rates.

Algae

The previous model version simulated phytoplankton into four general algal communities or groups: (1) bacillariophyta and crysophyta (diatoms); (2) chlorophyta (green algae); (3) cyanophyta (blue-green algae); and, (4) haptophyta and cryptophyta (flagellates). For this previous version, the paradigm of four general algal communities or groups was pursued rather than a more diverse modeling regime. Algal group dynamics within CE-QUAL-W2 models are sensitive and the uncertainty in model parameterization beyond four different algal groups can be problematic (Cole and Wells, 2015).

For the updated model, the cyanophyta group has been divided into two groups: a nitrogen-fixing cyanophyta group, generally representative of *Anabaena*, *Dolichospermum*, and *Cylindrospermopsis*, and a non-fixing, buoyant cyanophyta group, generally representative of *Planktothrix*, *Microcystis*, and *Woronichinia*. This enhancement was added to improve the

model's predictive capacity of cyanophyta (also known as cyanobacteria) blooms and focus on populations known to exist in Madison Lake. As the original model and the measured 2014 algal and chlorophyll *a* data suggested, a mid- to late-summer dominance by cyanophyta existed in 2014 and again in 2016. Furthermore, an analysis of algal data going back to 2013 suggested cyanophyta dominance in the mid- to late-summer months (Minnesota Pollution Control Agency, 2018).

However, as noted above, simulating beyond three to four algal groups within CE-QUAL-W2 can be challenging. The model updates to the algal community sub-module required substantial adjustments to many of the parameters governing algal growth and senescence for all five groups. Also, the lack of measured Madison Lake algal data beyond algal counts and biomass did not adequately constrain model parameterization independently. Instead, the guidance for determining algal growth patterns was mainly provided by other CE-QUAL-W2 modeling efforts, such as the previous sentinel lake models (Smith and others, 2014; Smith and others, 2017) and the Lake St. Croix CE-QUAL-W2 model (Smith and others, 2018).

Similar to the original model, the zooplankton grazing dynamics were captured within algal specific constants such as the algal growth rate (parameter AG) and the algal mortality rate (parameter AM) (Smith, 2019). Algal growth temperature ranges (parameters AT1 through AT4) were different across all five algal groups, as were the algal growth rates (parameter AG) and the light saturation intensities at the maximum photosynthetic rate (parameter ASAT). One major change from the original Madison Lake model was the fraction of algal growth specific to temperature ranges (parameters AK1 through AK4). Rather than adjust these parameters to artificially attain a better model fit, these parameters were set to the CE-QUAL-W2 default rates, given the lack of further information on these parameters. Other algal growth parameters were

also set with more uniformity across the different groups, given the lack of specific information for the Madison Lake algal groups. With the updated model, the stoichiometric equivalences used for determining the nutrients in the algal biomass, such as phosphorus, nitrogen, and carbon, were also set with more uniformity across the different algal groups and generally closer to the CE-QUAL-W2 default rates. Most importantly, the ratio between algal biomass and chlorophyll *a* was adjusted to 0.05 across all groups rather than different ratios between the groups, and this same adjustment was made for the transformation of the measured algal data conversions to biomass. For the original model, this parameterization was out of sync between both the different groups and the measured data.

Overall, the simulated distribution of the five algal groups (fig. 6), instead of four algal groups, was improved for the updated Madison Lake model from the original model (Smith and others, 2017). The algae MAE and RMSE values were generally not as meaningful statistics for calibration and validation; however, the MAE and RMSE values dropped across all of the five algal groups compared to the algal group simulations for the original model. The largest change in the MAE/RMSE values was for cyanophyta. In the original report, cyanophyta (referred to as “blue-green algae”) had MAE and RMSE values of 1.81 and 1.95 mg/L, respectively, whereas the updated model split this group into two groups with MAE and RMSE values <1.1 mg/L.

Figure 6. Simulated and measured algal group distributions (diatoms, green algae, fixing cyanophyta, non-fixing (buoyant) cyanophyta, and flagellates) for the 1-meter depth at Madison Lake southwest deep point near Madison Lake, Minn., May 15 to November 1, 2014.

For the 2014 calibration year, diatoms were the first group to peak, as shown with the simulated and measured values. Diatoms commonly peak earlier in the year (Sigeo, 2005). The simulated diatom values peaked by the middle of May and then approached 0 mg/L by late June.

For the measured values, a second peak occurred in late July and again in mid-September; however, the model did not capture these dynamics. Several factors controlled the lack of simulated diatom growth beyond early June. Simulated algal growth favored the other groups beyond the early part of the year. The temperature range for diatom growth was lower than the other algal groups, so once the lake warmed by early June, the diatoms were outcompeted by the other algal groups. The larger algal light saturation intensity for diatoms, which affected optimal algal growth, limited growth once the lake had greater concentrations of inorganic and organic suspended sediments, macrophytes, and algal biomass and thereby blocked the light. Combined with a larger settling rate, the diatoms would settle to a depth in the lake unfavorable for optimal light saturation set in the model.

The next group to succeed diatoms in 2014 were the fixing cyanophyta (fig. 6). As mentioned in the first Madison Lake modeling report, splitting up cyanophyta into at least two groups was warranted since the lake's nitrogen limitation at this time of year combined with warmer temperatures favored cyanophyta capable of fixing nitrogen. As less emphasis was placed on other factors compared to the original model, the wider temperature range for maximum algal growth (between 20 and 30 °C) combined with a lower algal light saturation intensity of 75 watts per square meter (W/m^2) compared to 120 W/m^2 for the diatoms allowed for more growth of fixing cyanophyta (*Anabaena*, *Dolichospermum*, and *Cylindrospermopsis*).

By mid-July, the light saturation and favorability for fixing cyanophyta growth began to wane in favor of the non-fixing cyanophyta group (*Planktothrix*, *Microcystis*, and *Woronichinia*). This algal group was also differentiated from the fixing cyanophyta group through a higher light saturation intensity (125 W/m^2) and for high buoyancy by adjusting the settling rate to 0. Throughout the remainder of the summer into September and October, the non-fixing

cyanophyta continued to grow, whereas the fixing cyanophyta group died off. The data supported this simulated growth, except the cyanophyta continued to have higher biomass in September for the measured data. This differentiation was difficult to simulate in the 2014 calibration, but for the 2016 validation the dynamics seemed to be closer to the measured data.

The other two algal community groups, green algae and flagellates, had similar growth rates and patterns for the simulated and measured values in 2014. The two groups were distinguished from each other in that the green algae showed a mid-August peak, whereas the flagellates showed a September peak (fig. 6). The maximum algal growth temperature range was similar for both groups, with 20 to 25 °C and 24 to 28 °C for the green algae and flagellates, respectively. Of the five groups, the flagellates had the lowest algal light saturation intensity of 20 W/m². Otherwise, as shown in the CE-QUAL-W2 control file (Smith, 2019), the parameterization of the two groups was similar for growth rate, algal mortality (parameter AM), and algal settling rate; and both groups had the same algal half-saturation constants for nitrogen- and phosphorus-limited growth (parameter AHSP).

Overall, the simulated algal biomass concentrations for the calibration were similar to measured algal biomass concentrations with the exception of the previously described deviation for diatoms later in the year. Also, the simulated cyanophyta concentrations did not match the large measured values in August and September, although the combined simulated growth of the fixing and non-fixing cyanophyta groups did match the measured values. Part of the likely discrepancy is that isolated sample points in time might not capture the general trend.

Figure 7. Simulated and measured chlorophyll a concentrations for the 1-meter depth at Madison Lake southwest deep point near Madison Lake, Minn. (segment 7) in Madison Lake, May 15 to November 1, 2014.

The chlorophyll *a* concentration data were used to help interpret if the overall magnitude of the algal group composition was in the correct range. Photosynthetic pigments, such as chlorophyll *a*, are accepted in the literature as surrogates for algal biomass given the large expense of measuring algal biomass directly (Lindenberg and others, 2008). Simulated and measured values of the chlorophyll *a* concentrations are shown for the Madison Lake southwest deep point site in figure 7 (segment 7, fig. 1). Measured chlorophyll *a* data were collected in the surface layer at approximately 1 m below the water surface as part of the monthly MNDNR water-quality sampling trips. Overall, the simulated values were a good approximation of the measured values, with the exception of the high simulated chlorophyll *a* value compared to the low measured chlorophyll *a* concentration in October.

Considerable differences occurred for the 2016 validation for both algal growth (fig. 8) and chlorophyll *a* (fig. 9). Unlike 2014, the simulated growth of green algae and flagellates occurred much earlier in the year than suggested by the measured data (fig. 8). Simulated diatom growth did occur, but at a much lower rate than 2014. The two cyanophyta groups also started to grow earlier in the year, but this growth was also supported by the measured data. The simulated fixing cyanophyta peaked in August at the same time as the measured fixing cyanophyta, whereas the non-fixing (buoyant) cyanophyta showed the same growth curve as 2014 except with an earlier start. The simulated non-fixing cyanophyta overall seemed to grow faster than the measured non-fixing cyanophyta, but this could also be due to a model limitation. The CE-QUAL-W2 model in general might have a difficult time distinguishing different nitrogen sources (organic versus non-organic sources), and in reality, the fixing cyanophyta group does not necessarily fix nitrogen at all times since nitrogen fixation is a highly energetic process (Maier, 2004). Within the CE-QUAL-W2 modeling framework, it is not possible to have the same group

set-up as using nitrogen fixation only part of the time, so this interplay of nitrogen fixation versus non-nitrogen fixation among different cyanophyta groups can be difficult to model. As with 2014, the chlorophyll *a* concentration data were used to help interpret if the overall magnitude of the algal group composition was in the correct range for 2016. Similar to 2014, the general trend was captured by the simulated chlorophyll *a* values but were lower than the measured data in the later summer mainly because the model did not capture the high measured non-fixing cyanophyta growth.

Figure 8. Simulated and measured algal group distributions (diatoms, green algae, fixing cyanophyta, non-fixing (buoyant) cyanophyta, and flagellates) for the 1-meter depth at Madison Lake southwest deep point near Madison Lake, Minn., March 30 to November 23, 2016.

Figure 9. Simulated and measured chlorophyll *a* concentrations for the 1-meter depth at Madison Lake southwest deep point near Madison Lake, Minn. (segment 7) in Madison Lake, March 30 to November 23, 2016.

Macrophyte Growth

The macrophyte growth model was run for the 2014 calibration and 2016 validation, given the high amount of documented macrophyte growth for Madison Lake (Lindon and others, 2010). As noted in Smith and others (2017), most of the macrophyte growth parameters were kept at default rates except for the maximum macrophyte growth rate (MG), the light saturation intensity at maximum photosynthetic rate (MSAT), and the fraction of macrophyte biomass that is converted to particulate organic matter after macrophytes die (MPOM). Additionally, two adjustments were made to the macrophyte growth module from the original Madison Lake CE-QUAL-W2 model. For the original model (Smith and others, 2017), the fractions of phosphorus

(PSED) and nitrogen uptake (NSED) from sediments were set equal to 1, but for the updated model both parameters were adjusted to 0.5.

Nutrients

Nutrients are controlled by many processes, such as inflow loads, algal production, and organic matter decay rates (Cole and Wells, 2015). One of the most important controls is the amount of nutrients (loads, determined in the model as concentration multiplied by streamflow and a unit conversion factor) contributed by the inflows, which are different for both lakes. Madison Lake had a larger flux of nitrate earlier in 2014 season with a larger flux of ammonia later in the year, whereas in 2016 for the model validation the lake did not have the initial large flux of nitrate mid-summer or the large mid-summer flux of ammonia. It is known that loading into lakes such as Madison Lake would be expected to vary across ecoregions, with the soil fertility in the contributing drainage basin, and across different land uses (for example, row-crop agriculture compared to deciduous forest). However, the data suggested interannual variability that the model must be able to account for to reasonably simulate the nutrient conditions.

In-lake processing of the nutrients is the major factor controlling nutrient concentrations. An in-depth discussion of the sources and sinks for Madison Lake was given in Smith and others (2017). In summary, Madison Lake has fairly small flows from two different inflows and seems to have considerably large groundwater sources relative to surface inflows. Agricultural land use is the dominant land use at approximately 50 percent for the drainage areas for Madison Lake with only 2 percent forest cover (Lindon and others, 2010), and the drainage basin to lake area ratio for Madison Lake is 4:1. Generally, basins with a smaller percentage of forest or other undeveloped land cover combined with a larger ratio of agricultural land use will have higher nutrient loads (U.S. Geological Survey, 1999).

As with water temperature and dissolved oxygen, new comparisons were warranted to make sure that the updated model still adequately captured the lake's nutrient dynamics for 2014 despite earlier calibration efforts (Smith and others, 2017). The focus for evaluating the model calibration and validation was three constituents of nitrogen and two constituents of phosphorus: nitrate plus nitrite, ammonia, total Kjeldahl nitrogen, orthophosphate, and total phosphorus. For purposes of comparing simulated and measured concentrations, total Kjeldahl nitrogen was classified as the concentration of nitrogen present in ammonia, nitrate plus nitrite, and organically bound nitrogen (in living algal biomass and all organic matter pools). For purposes of comparing simulated and measured concentrations, total phosphorus was classified as the concentration of phosphorus present in orthophosphate and bound up in organic matter (in living algal biomass and all organic matter pools). The primary tools for evaluating the degree of fit for the nutrients were the MAE and RMSE values (table 5) and all comparisons were for samples taken either from 1 m below the water surface or in the hypolimnion from the southwest deep point in Madison Lake (segment 7, fig. 1). It is worth noting that these values could often be largely offset by only one or two measured samples because of the small number of total discrete samples (five samples for 2014; 4-10 samples for 2016, depending on the constituent).

Dissolved ammonia and dissolved nitrate plus nitrite distributions in Madison Lake were largely affected by the inflows and the lake hydrodynamics. Few differences between the simulated and measured dissolved ammonia concentrations were noted at the 1-m depth from July through September, both for the calibration year (2014 – fig. 11) and the validation year (2016– fig. 12). An exception occurred for the June and October 2014 samples, which were both much higher than all the other samples. Overall, algal uptake of available ammonia was fairly rapid in the simulation and actual lake for both years, with replenishment by organic matter

decay and inflows. This process of algal uptake accounted for the lower dissolved ammonia concentrations during the middle of the simulation period for the simulated and measured values. The 2014 MAE and RMSE values for dissolved ammonia were comparable between the old calibration (Smith and others, 2017) and the new calibration (this report), with MAE and RMSE values of 0.17 and 0.33 mg/L, respectively (fig. 10; table 5), for the new calibration. The 2016 validation closely matched the measured values, which were all at the sample detection limit; the MAE and RMSE values for the 2016 validation were 0.01 and 0.02 mg/L, respectively.

Figure 10. Simulated and measured dissolved ammonia concentrations at 1 meter below the water surface in model segment 7 containing the Madison Lake southwest deep point near Madison Lake, Minn., May 15 to November 1, 2014, with values of mean absolute error (MAE) and root mean square error (RMSE).

Figure 11. Simulated and measured dissolved ammonia concentrations at 1 meter below the water surface in model segment 7 containing the Madison Lake southwest deep point near Madison Lake, Minn., March 30 to November 23, 2016, with values of mean absolute error (MAE) and root mean square error (RMSE).

Simulated and measured dissolved nitrate plus nitrite concentrations are shown in figures 12 (2014) and figure 13 (2016) for the Madison Lake southwest deep point site. For nitrate, the two years were very different: in 2014, nitrate started with a high initial value whereas 2016 started relatively low. The model simulated both years with very low MAE and RMSE values (table 5), including a drop in the MAE/RMSE values with the new 2014 calibration. The improvement was due in part to an important change to the NO₃S parameter which controls the nitrate sediment diffusion rate. Additionally, changes were made across the five algal groups to

the algal stoichiometry and also updates to the algal growth rates; all of these changes would affect dissolved nitrate and nitrite concentrations.

Figure 12. Simulated and measured dissolved nitrate plus nitrite concentrations at 1 meter below the water surface in model segment 7 containing the Madison Lake southwest deep point near Madison Lake, Minn., May 15 to November 1, 2014, with values of mean absolute error (MAE) and root mean square error (RMSE).

Figure 13. Simulated and measured dissolved nitrate plus nitrite concentrations at 1 meter below the water surface in model segment 7 containing the Madison Lake southwest deep point near Madison Lake, Minn., March 30 to November 23, 2016, with values of mean absolute error (MAE) and root mean square error (RMSE).

Dissolved orthophosphate concentrations in the Madison Lake measured data were relatively stable for both years (fig. 14; fig. 15), except a higher measured value in October 2014. The simulated orthophosphate concentrations were considerably more variable due to the algal dynamics incorporated into the model and the cycling of nutrients through the various organic pools, algal communities, and the lake's simulated macrophyte community. At the end of both the calibration (2014) and validations (2016) runs, a steady increase in simulated dissolved orthophosphate concentrations occurred primarily because of the lack of demand by the simulated algae and macrophytes. Overall, the MAE and RMSE values were 0.02 and 0.02 mg/L, respectively, for both years (fig. 14; fig. 15; table 5).

Figure 14. Simulated and measured dissolved orthophosphate concentrations at 1 meter below the water surface in model segment 7 containing the Madison Lake southwest deep point near Madison Lake,

Minn., May 15 to November 1, 2014, with values of mean absolute error (MAE) and root mean square error (RMSE).

Figure 15. Simulated and measured dissolved orthophosphate concentrations at 1 meter below the water surface in model segment 7 containing the Madison Lake southwest deep point near Madison Lake, Minn., March 30 to November 23, 2016, with values of mean absolute error (MAE) and root mean square error (RMSE).

Simulated and measured concentrations are shown for total Kjeldahl nitrogen in figures 16 and 17. The 2014 MAE and RMSE values for total Kjeldahl nitrogen were 0.35 and 0.43 mg/L, respectively (fig. 16; table 5), slightly higher than the original calibration (Smith and others, 2017) of 0.29 and 0.33 mg/L, respectively, for MAE and RMSE. The measured data indicate a dynamic range, from approximately 1.4 to 2.2 mg/L. A peak in total Kjeldahl nitrogen for the simulated values occurred in late June because of the increase in ammonia and nitrate concentrations, with a steady increase from late July through mid-September due to an accumulation in organic matter from the deterioration of algal biomass, macrophytes, and inflows. The simulated results were generally the same pattern as the measured total Kjeldahl nitrogen concentrations, except for a steady decrease in total Kjeldahl nitrogen towards the end of the simulation period (fig. 16). For the 2016 validation, the model fit was improved over the 2014 calibration with MAE and RMSE values of 0.20 and 0.24 mg/L, respectively. The simulated total nitrogen tracks the measured values throughout the simulation, and includes the same late season decline. These decreases were likely because of the overall decay of the simulated organic matter pools and the decrease in simulated total algal biomass.

Figure 16. Simulated and measured total Kjeldahl nitrogen concentrations at 1 meter below the water surface in model segment 7 containing the Madison Lake southwest deep point near Madison Lake, Minn., May 15 to November 1, 2014, with values of mean absolute error (MAE) and root mean square error (RMSE).

Figure 17. Simulated and measured total Kjeldahl nitrogen concentrations at 1 meter below the water surface in model segment 7 containing the Madison Lake southwest deep point near Madison Lake, Minn., March 30 to November 23, 2016, with values of mean absolute error (MAE) and root mean square error (RMSE).

Total phosphorus (fig. 18; fig. 19) is shown for the epilimnion and hypolimnion locations since measured hypolimnion values were available for total phosphorus. In the epilimnion, the measured total phosphorus concentrations were stable but the simulated concentrations for both the calibration (fig. 18) and validation (fig. 19) were too large. The model could have been fit to match the epilimnion concentrations better but would have sacrificed the hypolimnion phosphorus model fit with measured values and would have set phosphorus at unrealistically low stoichiometric equivalents for algal biomass and organic matter. In the hypolimnion, a steady and steep increase in the simulated total phosphorus occurred from late May until mid-September to greater than 1,200 $\mu\text{g/L}$, before crashing to the baseline of less than 150 $\mu\text{g/L}$. These high values were confirmed for both years with the measured data, with a high value of 1,130 $\mu\text{g/L}$ in 2014 and 815 $\mu\text{g/L}$ in 2016. The likely explanation for the large phosphorus concentrations in the simulated and measured values (fig. 18; fig. 19) was the large release rates in phosphorus from the lake sediments. The MAE values for the epilimnion (1-m depth) and hypolimnion (15.5-m depth or 16.5-m depth) were 82 and 54 $\mu\text{g/L}$, respectively; the RMSE

values for the epilimnion (1-m depth) and hypolimnion (16.5-m depth) were 86 and 69 $\mu\text{g/L}$, respectively (fig. 26; table 5). The large drop in total phosphorus coincides with the turnover of Madison Lake and the mixing of all the lake water, which redistributed the concentrated total phosphorus to the entire lake volume.

Figure 18. Simulated and measured total phosphorus concentrations at 1 meter and 16.5 meters below the water surface in model segment 7 containing the Madison Lake southwest deep point near Madison Lake, Minn., May 15 to November 1, 2014, with values of mean absolute error (MAE) and root mean square error (RMSE).

Figure 19. Simulated and measured total phosphorus concentrations at 1 meter and 15.5 meters below the water surface in model segment 7 containing the Madison Lake southwest deep point near Madison Lake, Minn., March 30 to November 23, 2016, with values of mean absolute error (MAE) and root mean square error (RMSE).

Phosphorus Loads

Monthly total phosphorus budgets were calculated for the updated Madison Lake model for 2014 and 2016 (table 6), and included phosphorus subdivisions of external phosphorus load derived from organic matter, external phosphorus load derived from orthophosphate, and internal phosphorus load released by zero-order sediment release. Additionally, monthly phosphorus budgets were calculated for the original Madison Lake model (Smith and others, 2017) and two sensitivity analyses completed in the same report, both with a 20 percent variation in the incoming dissolved orthophosphate load (20 percent increase, 20 percent decrease). Phosphorus budgets included external sources from the two tributaries, the distributed tributary flow (unaccounted surface flow, groundwater flow), and internal phosphorus loading from sediment

release. Negative numbers in the table denote a loss term due to net export of phosphorus for the distributed tributary flow.

Table 6. Summary of phosphorus loading for updated Madison Lake model (2014, 2016), original Madison Lake model, and two phosphorus loading scenarios, according to load estimates and internal CE-QUAL-W2 calculations. Negative terms denote a loss term due to the net export of phosphorus (from the distributary tributary flow).

In comparisons between the 2014 and 2016 model runs (updated model), the 2016 model simulation had a higher overall total phosphorus budget. Even if only considering the periods of overlap (May through October), 2016 had approximately 25 percent more total phosphorus loading than 2014. More precipitation, and therefore higher flows, occurred for 2016 than 2014, and was the primary driver of the increased loads as the limited concentration data for the two different years were similar (Smith, 2019). When comparing the monthly data, the highest 2014 phosphorus loads occurred in June (2,750 kilograms) before dropping throughout the rest of the summer (fig. 20), whereas the 2016 monthly phosphorus loads stayed relatively high from June to October (range: 856 to 1,783 kilograms per month). Most of the load for the remainder of 2014 after August was internal loading, since there was little to no flow into Madison Lake after early September.

Figure 20. Total phosphorus concentrations monthly, in kilograms per month, for the 2014 and 2016 model years for the updated model.

For the other three model runs (scenarios 3-5; table 6), the original 2014 model was included to show that there was relatively little difference in the phosphorus budget between the original and updated model. For the sensitivity scenario increasing the external dissolved

orthophosphate load by 20 percent (scenarios 4; table 6), as compared to the original model (scenario 3; table 6), increasing this external load did increase the overall phosphorous load by approximately 7 percent (5,596 kilograms versus 5,244 kilograms). Alternatively, decreasing the external dissolved orthophosphate load by 20 percent (scenarios 5; table 6) decreased the total phosphorus load by approximately 7 percent (4,904 kilograms versus 5,244 kilograms).

As a percentage of the overall load, the internal sediment release of phosphorus accounted for between 39 to 48.1 percent of the model run load (table 6). On a month-by-month basis, the internal load covers a much wider range, ranging from almost no internal sediment release of phosphorus to dominating the overall monthly load. The high percent of internal load is particularly high in the summer months when hypoxic conditions dominated the lake's hypolimnion, with low release rates occurring before hypoxia dominates the lake or after the fall lake mixing. Little difference existed between the total internal load for 2014 and 2016 (scenarios 1-2; table 6), relative to the large differences from external loads.

Model Limitations

A full understanding of model limitations is necessary to better evaluate the performance of any water-quality model. The previous Madison Lake CE-QUAL-W2 model report elaborated further on these limitations, but it is important to reiterate the limitations due to the limited datasets available for Madison Lake. The fixed number of water-quality samples to which the model is calibrated may not have captured the full range of conditions in the dynamic systems. Also, all boundary conditions datasets had limitations. Water-quality data were linearly interpolated between sampling dates. The continuous streamflow for both tributaries and one outflow location, based on applying the 2014 elevation-streamflow ratings (Smith and others,

2017 – appendix table 1–1) to continuous water levels, were unavailable for 2016 so instead these elevation-streamflow ratings were applied to the daily water-surface elevation for the lake. Inherent errors in this approach would be captured by the constructed distributary tributary flows, but this still represents an important limitation. Finally, the continuous water temperatures were also unavailable for 2016 so a substituted dataset relating air temperature to water temperature had to be substituted for the tributary inflows.

Another source of limitations was the lack of specific information on algal growth rates, mortality rates, sinking rates, and algal light saturation coefficients. Also, the full stoichiometric equivalences for the individual algal groups was not known for the Madison Lake phytoplankton. Incubation experiments on some of these parameters could help constrain model parameterization, rather than depending on a manual parameter estimation process. Literature values for these constants do exist, but they tend to show a wide range that only help constrain the parameter estimation process rather than fix the parameters to a single value. Overall, the model did show the ability to simulate the different algal groups throughout the year, but better characterization of the algal community dynamics from either field or laboratory experimentation would improve the model further.

Summary

A previously developed CE-QUAL-W2 model for Madison Lake, Minnesota, simulated the algal community dynamics, water quality, and fish habitat suitability of Madison Lake under recent (2014) meteorological conditions. Additionally, this earlier model simulated the complex interplay between external nutrient loading, internal nutrient loading from sediment release of phosphorus, and the organic matter decomposition of the algal biomass. However, the

partitioning of cyanobacteria within the modeling framework was simplified to one group and did not account for how different cyanobacteria populations are affected by light conditions, the usage of nitrogen, temperature growth ranges, and differences in settling rates. To get a better handle on the proliferation of cyanobacteria in Madison Lake, the model required updates to at least partition the cyanobacteria into a group that fixed nitrogen and a second, more buoyant cyanobacteria group, that did not independently fix nitrogen.

To address the shortcomings of simulating cyanobacteria in the earlier model, the U.S. Geological Survey (USGS), in cooperation with the St. Croix Watershed Research Station (Science Museum of Minnesota), updated the Madison Lake CE-QUAL-W2 model to better characterize cyanobacteria into two groups. In addition to updating the cyanobacteria group differentiation, the entire portion of the model that handles the simulation of algal community dynamics was updated while preserving the model's predictive capabilities for nutrients, water temperature, and dissolved oxygen. The calibration and validation of the model was done under recent meteorological conditions with large and persistent cyanobacteria blooms (2014 and 2016). Overall, the model simulations predicted the persistently large total phosphorus concentrations in Madison Lake's hypolimnion, key differences in nutrient concentrations between the two years, and cyanobacteria bloom persistence.

For calibration targets, the CE-QUAL-W2 model successfully predicted water temperature on the basis of the two metrics of mean absolute error and root mean square error. One of the main calibration tools for CE-QUAL-W2 model development was the vertical profile temperature data. Altogether, simulated Madison Lake water temperatures tracked measured water temperatures throughout the water column. In addition to water temperature, the CE-QUAL-W2 model successfully predicted dissolved oxygen concentration based on the same two

metrics of mean absolute error and root mean square error. Along with temperature, dissolved oxygen is a key metric to illustrate the accuracy of the model's calibration. Simulated vertical profiles of dissolved oxygen concentration generally matched the largest change in measured dissolved oxygen concentration, including the approximate depth, slope, and timing of large shifts.

Monthly total phosphorus budgets calculated for the updated Madison Lake model for 2014 and 2016 found that 2016 had significantly more internal and external phosphorus loading. Most of the additional phosphorus loading was from external inputs into Madison Lake rather than internal phosphorus release from sediments. The additional loading was likely from increased precipitation, and therefore higher flows, for 2016 as little to no inflow occurred into Madison Lake after September 2014. As a percentage of the overall load, the internal sediment release of phosphorus accounted for between 39 to 48.1 percent of the total external and internal phosphorus loads.

References Cited

American Water Works Association, American Public Works Association, and Water Environment Federation, 1997a, 4500-P phosphorus, *in* Rice, E.W., Baird, R.B., Eaton, A.D., and Clesceri, L.S., eds., *Standard methods for the examination of water and wastewater*: New York, American Water Works Association, American Public Works Association, and Water Environment Federation, p. 4-108–4-117.

American Water Works Association, American Public Works Association, and Water Environment Federation, 1997b, 10200-H chlorophyll, *in* Rice, E.W., Baird, R.B., Eaton, A.D., and Clesceri, L.S., eds., *Standard methods for the examination of water and wastewater*:

- New York, American Water Works Association, American Public Works Association, and Water Environment Federation, p. 10-18 – 10-25.
- American Water Works Association, American Public Works Association, and Water Environment Federation, 1997c, SM 2540C—Total dissolved solids dried at 180°C, *in* Rice, E.W., Baird, R.B., Eaton, A.D., and Clesceri, L.S., eds., Standard methods for the examination of water and wastewater: New York, American Water Works Association, American Public Works Association, and Water Environment Federation, p. 2–57.
- American Water Works Association, American Public Works Association, and Water Environment Federation, 1997d, 4500-SiO₂ C. molybdosilicate method, *in* Rice, E.W., Baird, R.B., Eaton, A.D., and Clesceri, L.S., eds., Standard methods for the examination of water and wastewater: New York, American Water Works Association, American Public Works Association, and Water Environment Federation, p. 4-156 – 4-158.
- Anderson, P., and Martin, I., 2015, Standard operating procedures (SOP)—Lake water quality sampling: Minnesota Pollution Control Agency, 17 p.
- Bales, J.D., and Robbins, J.C., 1999, A dynamic water-quality modeling framework for the Neuse River Estuary, North Carolina: U.S. Geological Survey Water-Resources Investigations Report 99–4017, 42 p. [Also available at <http://pubs.usgs.gov/wri/1999/4017/report.pdf>.]
- Cole, T.M., and Wells, S.A., 2015, CE-QUAL-W2—A two-dimensional, laterally averaged, hydrodynamic and water quality model, version 4.0: Portland State University Report, 847 p.
- Doman, A.M., Rucker, J., Pick, F.R., Fastner, J., Rohrlack, T., Mischke, U., and Wiedner, C., 2012, Cyanobacteria and cyanotoxins: the influence of nitrogen versus phosphorus: PLoS One, v. 7, 14 p. [Also available at <https://www.ncbi.nlm.nih.gov/pmc/articles/PMC3376147/>.]

- Fang, X., Stefan, H.G., and Alam, S.R., 1999, Simulation and validation of fish thermal DO habitat in north-central US lakes under different climate scenarios: *Ecological Modelling*, v. 118, no. 2–3, p. 167–191. [Also available at [http://dx.doi.org/10.1016/S0304-3800\(99\)00018-6](http://dx.doi.org/10.1016/S0304-3800(99)00018-6).]
- Flowers, J.D., Hauck, L.M., and Kiesling, R.L., 2001, USDA Lake Waco-Bosque River Initiative—Water quality modeling of Lake Waco using CE-QUAL-W2 for assessment of phosphorus control strategies: Texas Institute for Applied Environmental Research TR0114, 73 p.
- Galloway, J.M., and Green, W.R., 2006, Application of a two-dimensional reservoir water-quality model of Beaver Lake, Arkansas, for the evaluation of simulated changes in input water quality, 2001–2003: U.S. Geological Survey Scientific Investigations Report 2006–5302, 31 p. [Also available at <http://pubs.usgs.gov/sir/2006/5302/>.]
- Galloway, J.M., Ortiz, R.F., Bales, J.D., and Mau, D.P., 2008, Simulation of hydrodynamics and water quality in Pueblo Reservoir, southeastern Colorado, for 1985 through 1987 and 1999 through 2002: U.S. Geological Survey Scientific Investigations Report 2008–5056, 56 p. [Also available at <http://pubs.usgs.gov/sir/2008/5056/>.]
- Graham, J.L., Dubrovsky, N.M., and Eberts, S.M., 2016, Cyanobacterial harmful algal blooms and U.S. Geological Survey science capabilities: U.S. Geological Survey Open-File Report 2016-1174, 12 p.
- Green, W.R., Galloway, J.M., Richards, J.M., and Wesolowski, E.A., 2003, Simulation of hydrodynamics, temperature, and dissolved oxygen in Table Rock Lake, Missouri, 1996–1997: U.S. Geological Survey Water-Resources Investigations Report 2003–4237, 35 p. [Also available at <https://pubs.er.usgs.gov/publication/wri034237>.]

- Lindenberg, M.K., Hoilman, Gene, and Wood, T.M., 2008, Water quality conditions in Upper Klamath and Agency Lakes, Oregon, 2006: U.S. Geological Survey Scientific Investigations Report 2008–5201, 66 p. [Also available at <http://pubs.usgs.gov/sir/2008/5201/>.]
- Lindon, M., and Heiskary, S.A., 2007, Microcystin levels in eutrophic south central Minnesota lakes: Minnesota Lake Water Quality Assessment Series, 53 p. [Also available at <https://www.pca.state.mn.us/sites/default/files/wq-lar3-11.pdf>.]
- Lindon, M. and Heiskary, S., 2009, Blue-green algal toxin (microcystin) levels in Minnesota lakes: *Lake and Reservoir Management*, v. 25 (3), p. 240-252.
- Lindon, M., Valley, R., and Mackenthun, S., 2010, Sentinel lake assessment report—Madison Lake (07–0044), Blue Earth County, Minnesota: accessed May 11, 2016, at <https://www.pca.state.mn.us/sites/default/files/wq-2slice07-0044.pdf>.
- Loftin, K.A., Graham, J.L., Hilborn, E.D., Lehmann, S.C., Meyer, M.T., Dietze, J.E., and Griffith, C.B., 2016, Cyanotoxins in inland lakes of the United States: Occurrence and potential recreational health risks in the EPA National Lakes Assessment 2007: *Harmful Algae*, v. 56, p. 77-90.
- Maier, R.J., 2004, Nitrogen fixation and respiration: two processes linked by the energetic demands of nitrogenase, in Zannoni, D., ed., *Respiration in archaea and bacteria: advances in photosynthesis and respiration*: Dordrecht, Netherlands, Springer Publishing, p. 101-120.
- Merel, S., Walker, D., Chicana, R., Snyder, S., Baurès, E., and Thomas, O., 2013, State of knowledge and concerns on cyanobacterial blooms and cyanotoxins: *Environment International*, v. 59, p. 303-327.

Minnesota Department of Health, 2016, Environmental laboratory sampling and analysis guide:
accessed May 11, 2016, at

<http://www.health.state.mn.us/divs/phl/environmental/handbook.pdf>.

Minnesota Department of Natural Resources, 2016, Fisheries lake survey—Madison Lake:
accessed May 11, 2016, at

<http://www.dnr.state.mn.us/lakefind/showreport.html?downum=07004400>.

Minnesota Pollution Control Agency, 2018, Surface water data: Lake and stream water quality
assessment information [Madison: At Madison Lake (Town) (Lake)]: accessed June 21, 2019,
at <https://cf.pca.state.mn.us/water/watershedweb/wdip/waterunit.cfm?wid=07-0044-00>.

Minnesota Department of Natural Resources, 2019a, Lake Level Minnesota volunteering:
accessed June 21, 2019, at

<https://www.dnr.state.mn.us/climate/waterlevels/lakes/volunteering.html>.

Minnesota Department of Natural Resources, 2019b, Lake water level report—Madison Lake:
accessed May 25, 2019, at

<http://www.dnr.state.mn.us/lakefind/showlevel.html?downum=07004400>.

Minnesota Geospatial Information Office, 2016, Lake bathymetric outlines, contours, vegetation,
and DEM: accessed May 11, 2016, at <https://gisdata.mn.gov/dataset/water-lake-bathymetry>.

National Centers for Environmental Information, 2016, 1981-2010 station normals of
temperature, precipitation, and heating and cooling degree days (Mankato, MN, USA,
GHCND: USC00215073): National Oceanic and Atmospheric Administration, 4 p.

National Climatic Data Center, 2016, Climate data online: accessed May 11, 2016, at

<https://www.ncdc.noaa.gov/cdo-web/>.

National Climatic Data Center, 2018, Climate data online: accessed August 25, 2018, at <https://www.ncdc.noaa.gov/cdo-web/>.

O’Neil, J.M., Davis, T.W., Burford, M.A., and Gobler, C.J., 2012, The rise of harmful cyanobacterial blooms: The potential roles of eutrophication and climate change: *Harmful Algae*, v. 14, p. 313-334.

Paerl, H.W., and Otten, T.G., 2013, Harmful cyanobacterial blooms – causes, consequences, and controls: *Microbial Ecology*, v. 64, p. 995-1010.

PhycoTech, 2019, General technical approach (ASA): St. Joseph, Michigan, PhycoTech, Inc., 17 p. [Also available at <https://www.phycotech.com/Portals/0/PDFs/GenTech.pdf>.]

Preud’homme, E.B., and Stefan, H.G., 1992, Relationship between water temperatures and air temperatures for central U.S. streams: University of Minnesota St. Anthony Falls Hydraulic Laboratory Project Report No. 333, 143 p.

Rantz, S.E., and others, 1982a, Measurement and computation of streamflow—Volume 1. Measurement of stage and discharge: U.S. Geological Survey Water-Supply Paper 2175, v. 1, 313 p. [Also available at <http://pubs.usgs.gov/wsp/wsp2175/>.]

Rantz, S.E., and others, 1982b, Measurement and computation of streamflow—Volume 2. Computation of discharge: U.S. Geological Survey Water-Supply Paper 2175, v. 2, 373 p. [Also available from <http://pubs.usgs.gov/wsp/wsp2175/>.]

Sigeo, D.C., 2005, *Freshwater microbiology—Biodiversity and dynamic interactions of microorganisms in the aquatic environment*: West Sussex, England, John Wiley and Sons Ltd, 524 p.

Smith, E.A., Kiesling, R.L., Galloway, J.M., and Ziegeweid, J.R., 2014, Water quality and algal community dynamics of three sentinel deepwater lakes in Minnesota utilizing CE-QUAL-W2

models: U.S. Geological Survey Scientific Investigations Report 2014–5066, 73 p. [Also available at <http://dx.doi.org/10.3133/sir20145066>.]

Smith, E.A., Kiesling, R.L., and Ziegeweid, J.R., 2017, Water-quality models to assess algal community dynamics, water quality, and fish habitat suitability for two agricultural land-use dominated lakes in Minnesota, 2014: U.S. Geological Survey Scientific Investigations Report 2017–5056, 65 p. [Also available at <https://doi.org/10.3133/sir20175056>.]

Smith, E.A., Kiesling, R.L., Ziegeweid, J.R., Elliott, S.M., and Magdalene, Suzanne, 2018, Simulation of hydrodynamics, water quality, and lake sturgeon habitat volumes in Lake St. Croix, Wisconsin and Minnesota, 2013: U.S. Geological Survey Scientific Investigations Report 2017–5157, 60 p. [Also available at <https://doi.org/10.3133/sir20175157>.]

Smith, E.A., 2019, CE–QUAL–W2 water-quality model for Madison Lake, Minnesota, 2014 and 2016: U.S. Geological Survey data release, <https://doi.org/10.5066/XXXXXXXX>.

Sullivan, A.B., and Rounds, S.A., 2004, Modeling hydrodynamics, temperature, and water quality in Henry Hagg Lake, Oregon, 2000–03: U.S. Geological Survey Scientific Investigations Report 2004–5261, 38 p. [Also available at <http://pubs.usgs.gov/sir/2004/5261/>.]

Sullivan, A.B., Rounds, S.A., Deas, M.L., Asbill, J.R., Wellman, R.E., Stewart, M.A., Johnston, M.W., and Sogutlugil, I.E., 2011, Modeling hydrodynamics, water temperature, and water quality in the Klamath River upstream of Keno Dam, Oregon, 2006–09: U.S. Geological Survey Scientific Investigations Report 2011–5105, 82 p. [Also available at <http://pubs.usgs.gov/sir/2011/5105/>.]

- U.S. Environmental Protection Agency, 1993a, Method 353.2, revision 2.0—Determination of nitrate-nitrite nitrogen by automated colorimetry: Cincinnati, Ohio, U.S. Environmental Protection Agency, 14 p.
- U.S. Environmental Protection Agency, 1993b, Method 350.1—Determination of ammonia nitrogen by semi-automated colorimetry: Cincinnati, Ohio, U.S. Environmental Protection Agency, 12 p.
- U.S. Environmental Protection Agency, 1993c, Method 351.2, revision 2.0—Determination of total kjeldahl nitrogen by semi-automated colorimetry: Cincinnati, Ohio, U.S. Environmental Protection Agency, 15 p.
- U.S. Environmental Protection Agency, 1993d, Method 365.1, revision 2.0—Determination phosphorus by semi-automated colorimetry: Cincinnati, Ohio, U.S. Environmental Protection Agency, 15 p.
- U.S. Environmental Protection Agency, 2002, Guidelines establishing test procedures for the analysis of pollutants (Part 136, Appendix B. Definition and procedure for the determination of the method detection limit—Revision 1.11): U.S. Code of Federal Regulations, Title 40, revised as of July 1, 2002, p. 635–638.
- U.S. Environmental Protection Agency, 2007, Method 200.7—Trace elements in water, solids, and biosolids by inductively coupled plasma-atomic emission spectrometry: Cincinnati, Ohio, U.S. Environmental Protection Agency, 68 p.
- U.S. Geological Survey, 1999, The quality of our Nation's Waters—Nutrients and pesticides: U.S. Geological Survey Circular 1225, 82 p. [Also available at <http://pubs.usgs.gov/circ/circ1225/pdf/index.html>.]

U.S. Geological Survey, 2016, National Elevation Dataset: accessed May 11, 2016, at <http://ned.usgs.gov/>.

U.S. Geological Survey, 2019, National Water Information System—Web interface: accessed October 6, 2016, at <http://dx.doi.org/10.5066/F7P55KJN>.

Wetzel, R.G., 2001, Limnology lake and river ecosystems (3d ed.): San Diego, California, Elsevier, 1006 p.

Xu, Hai, Paerl, H.W., Qin, B., Zhu, G., and Gao, G., 2010, Nitrogen and phosphorus inputs control phytoplankton growth in eutrophic Lake Taihu, China: *Limnology and Oceanography*, v. 55, no. 1, p. 420–432. [Also available at <http://doi.org/10.4319/lo.2010.55.1.0420>.]

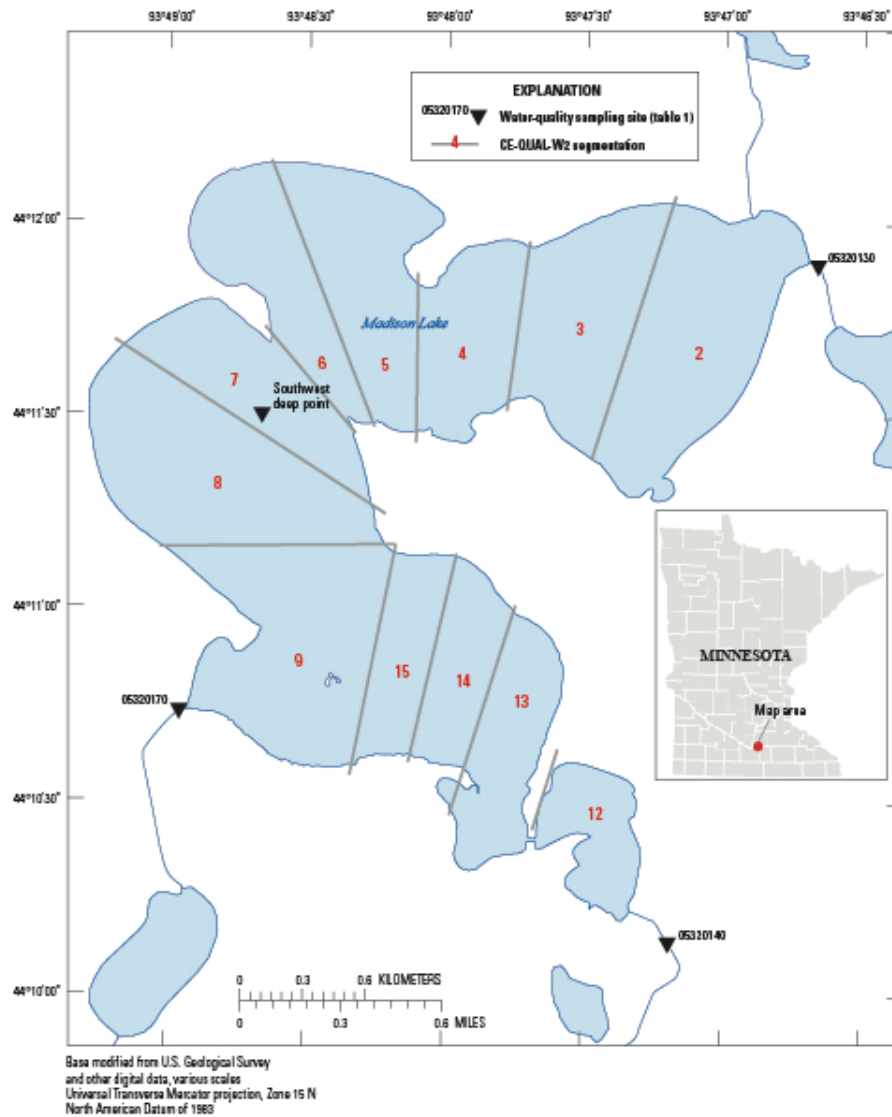


Figure 1: Map showing location of water-quality sampling sites for Madison Lake, Minnesota.

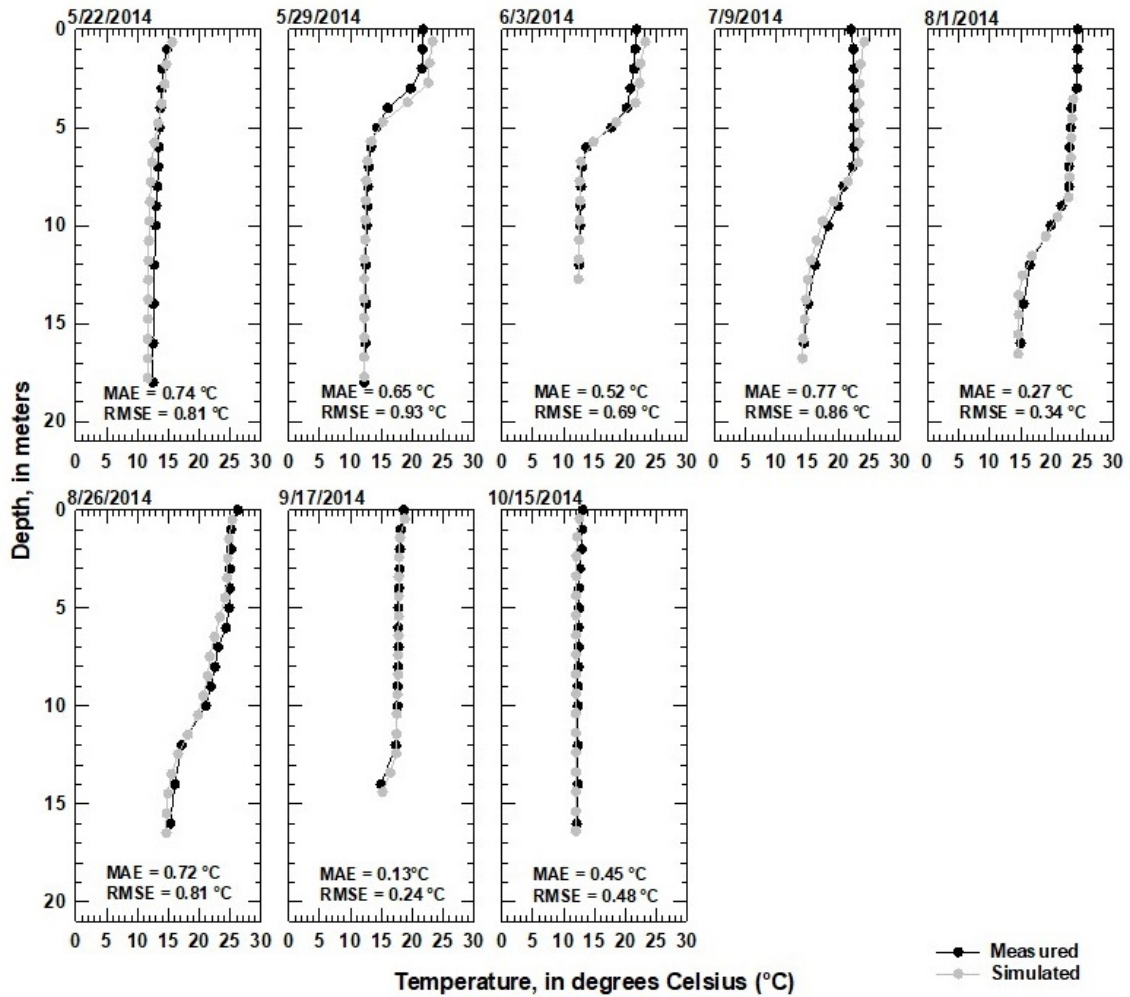


Figure 2: Simulated and measured water temperature for vertical profiles at Madison Lake southwest deep point near Madison Lake, Minn. for eight dates in 2014, with values of mean absolute error (MAE) and root mean square error (RMSE).

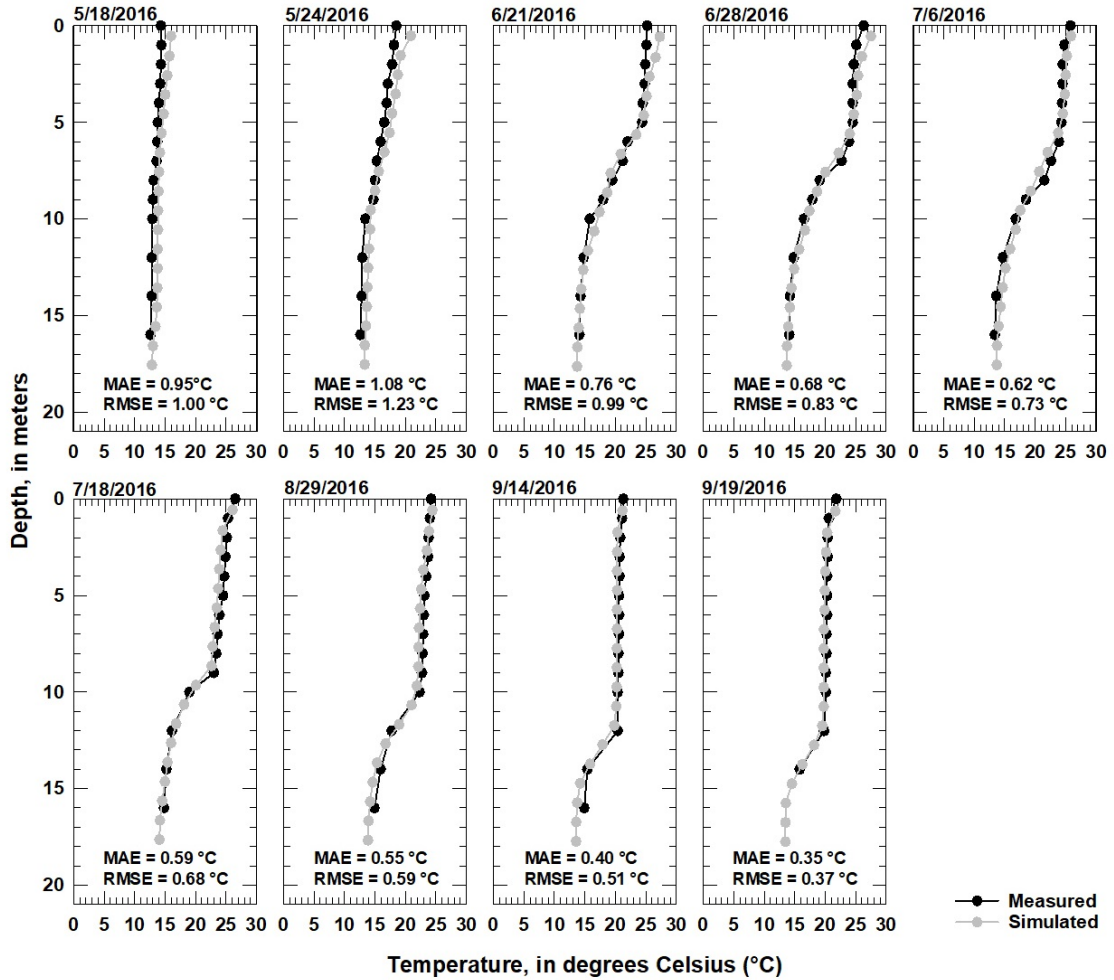


Figure 3: Simulated and measured water temperature for vertical profiles at Madison Lake southwest deep point near Madison Lake, Minn. for nine dates in 2016, with values of mean absolute error (MAE) and root mean square error (RMSE).

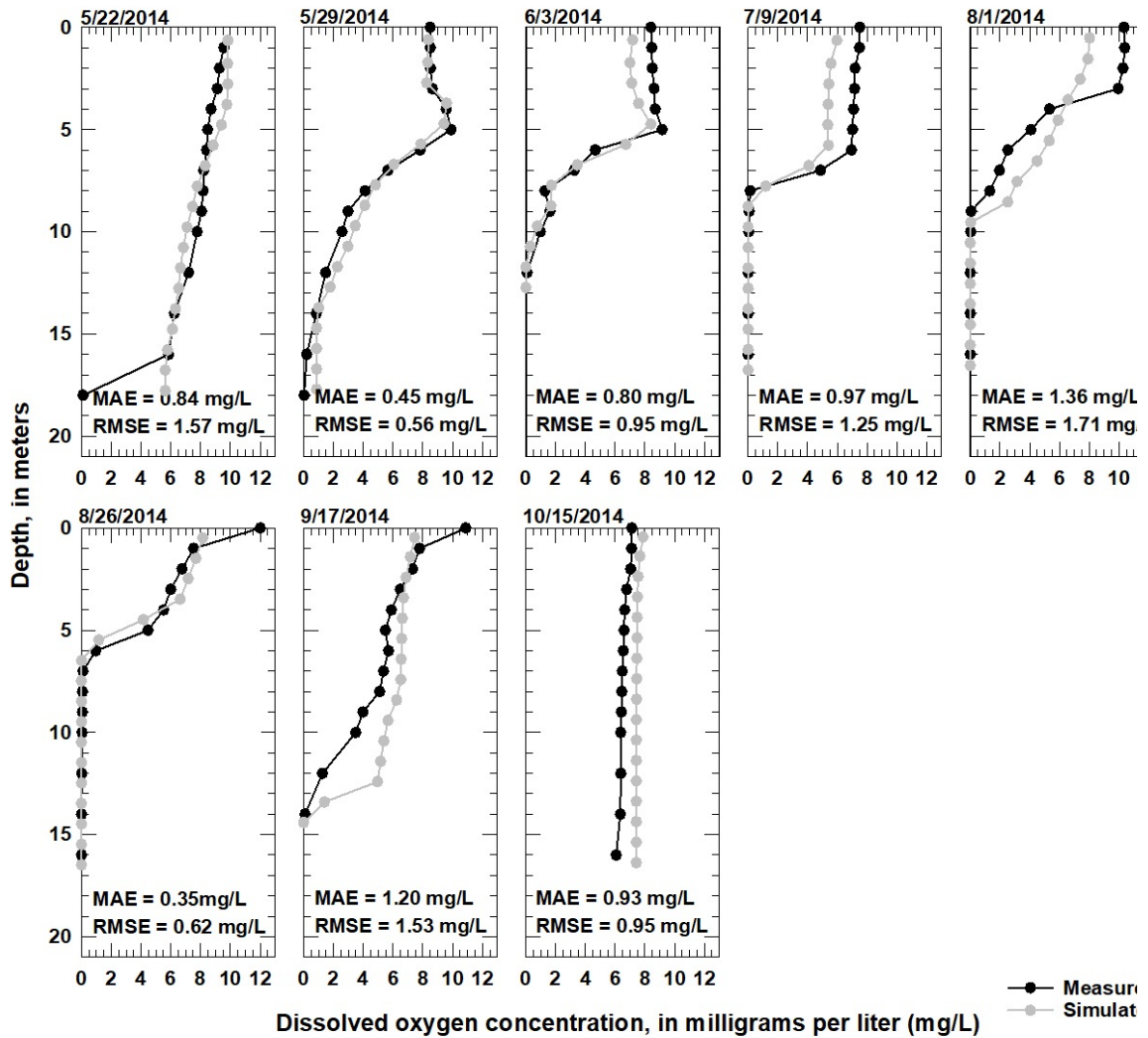


Figure 4: Simulated and measured dissolved oxygen concentration for vertical profiles at Madison Lake southwest deep point near Madison Lake, Minn. for eight dates in 2014, with values of mean absolute error (MAE) and root mean square error (RMSE).

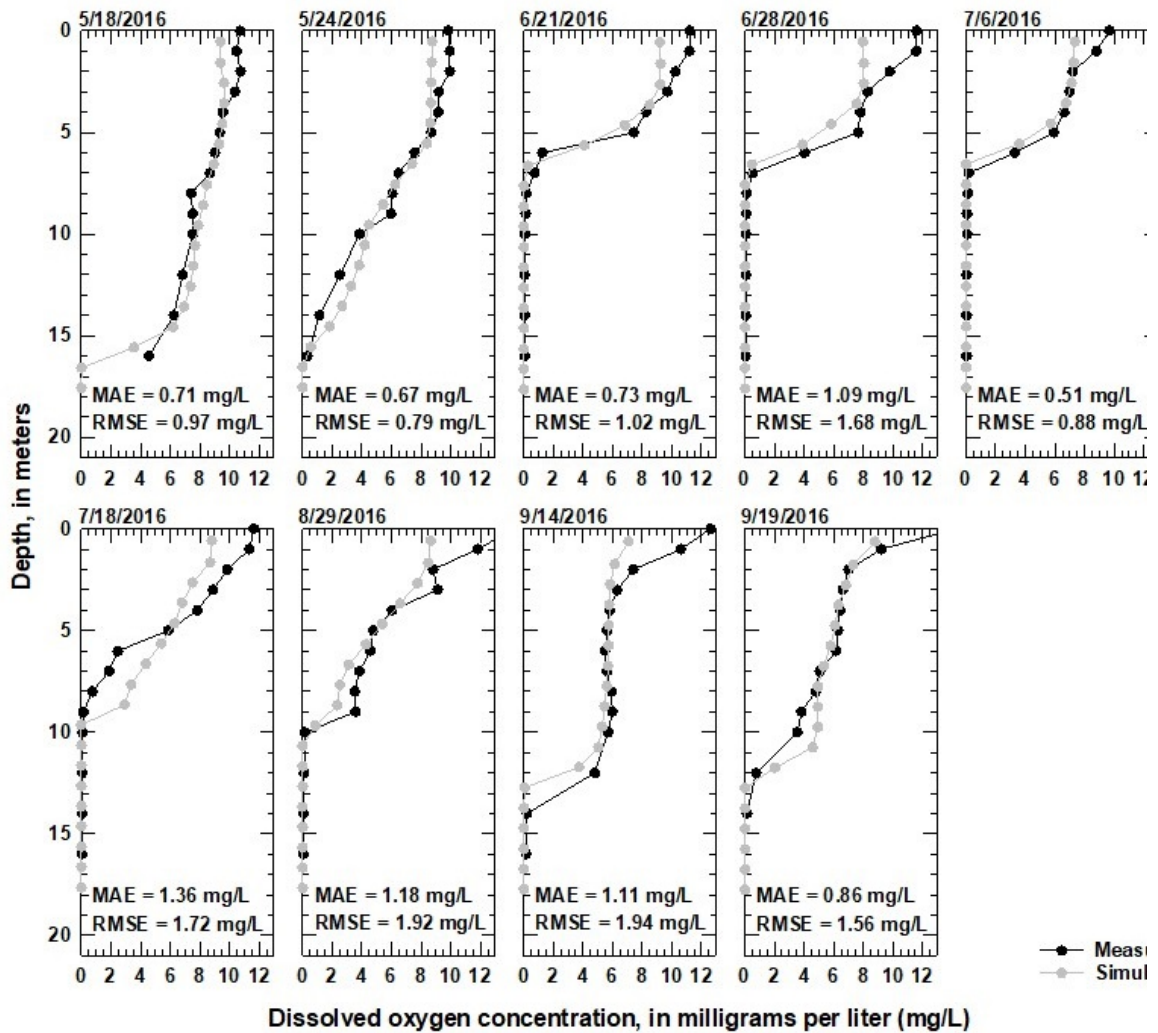


Figure 5: Simulated and measured dissolved oxygen concentration for vertical profiles at Madison Lake southwest deep point near Madison Lake, Minn. for nine dates in 2016, with values of mean absolute error (MAE) and root mean square error (RMSE).

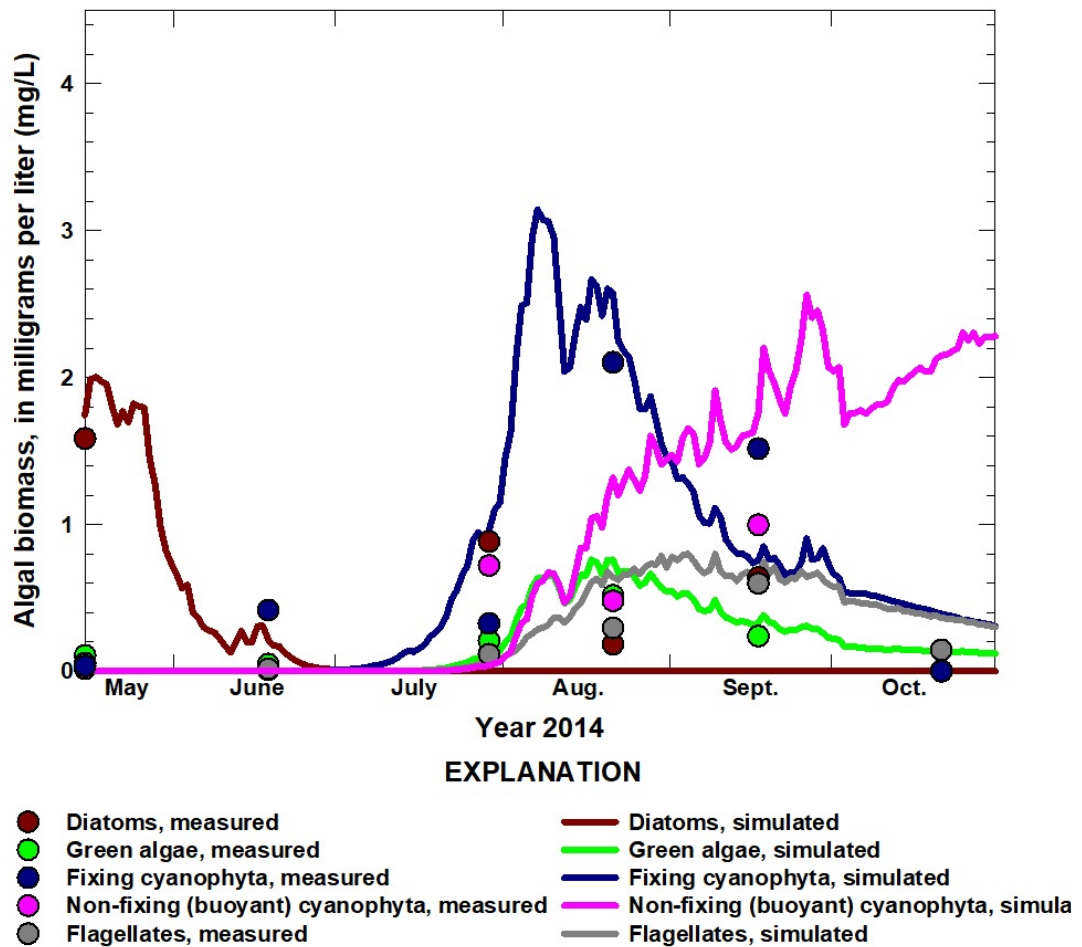


Figure 6: Simulated and measured algal group distributions (diatoms, green algae, fixing cyanophyta, non-fixing (buoyant) cyanophyta, and flagellates) for the 1-meter depth at Madison Lake southwest deep point near Madison Lake, Minn., May 15 to November 1, 2014.

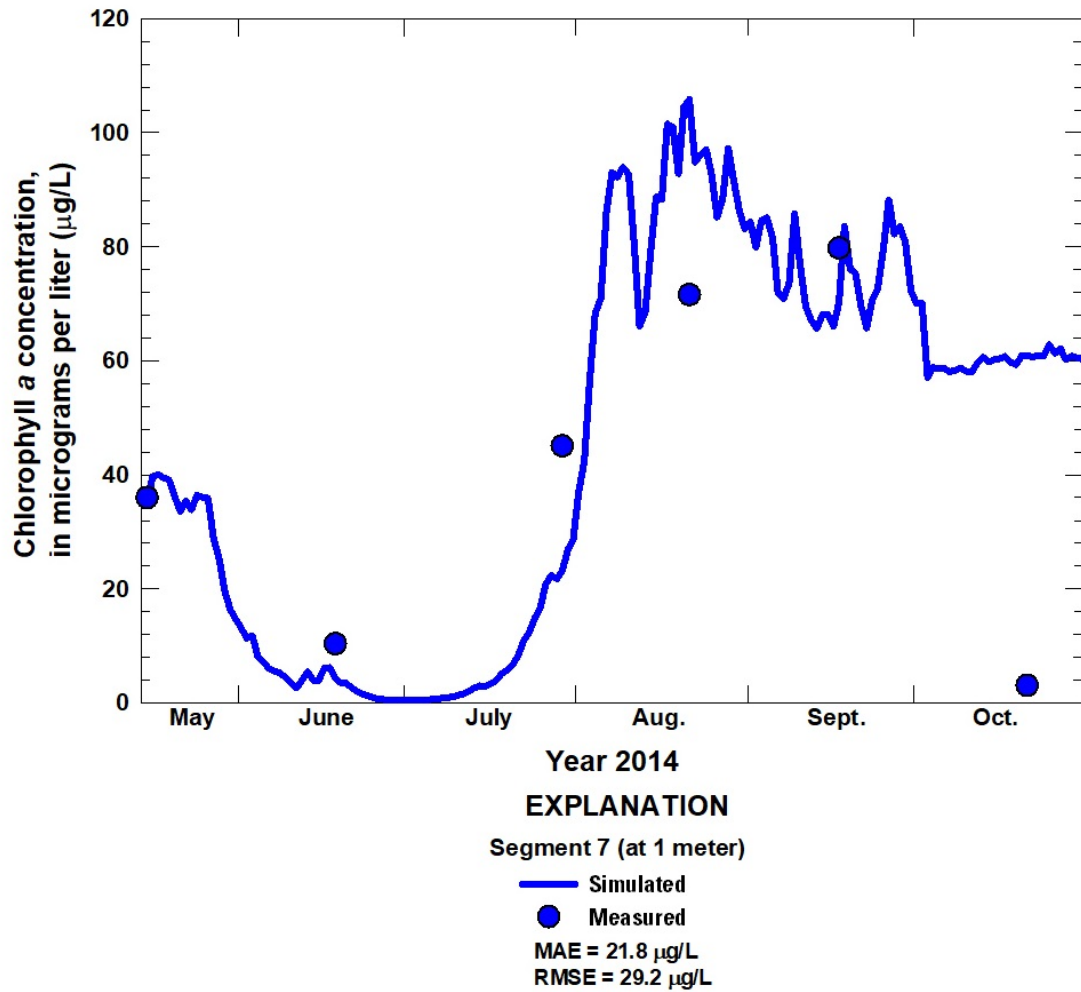


Figure 7: Simulated and measured chlorophyll *a* concentrations for the 1-meter depth at Madison Lake southwest deep point near Madison Lake, Minn. (segment 7) in Madison Lake, May 15 to November 1, 2014.

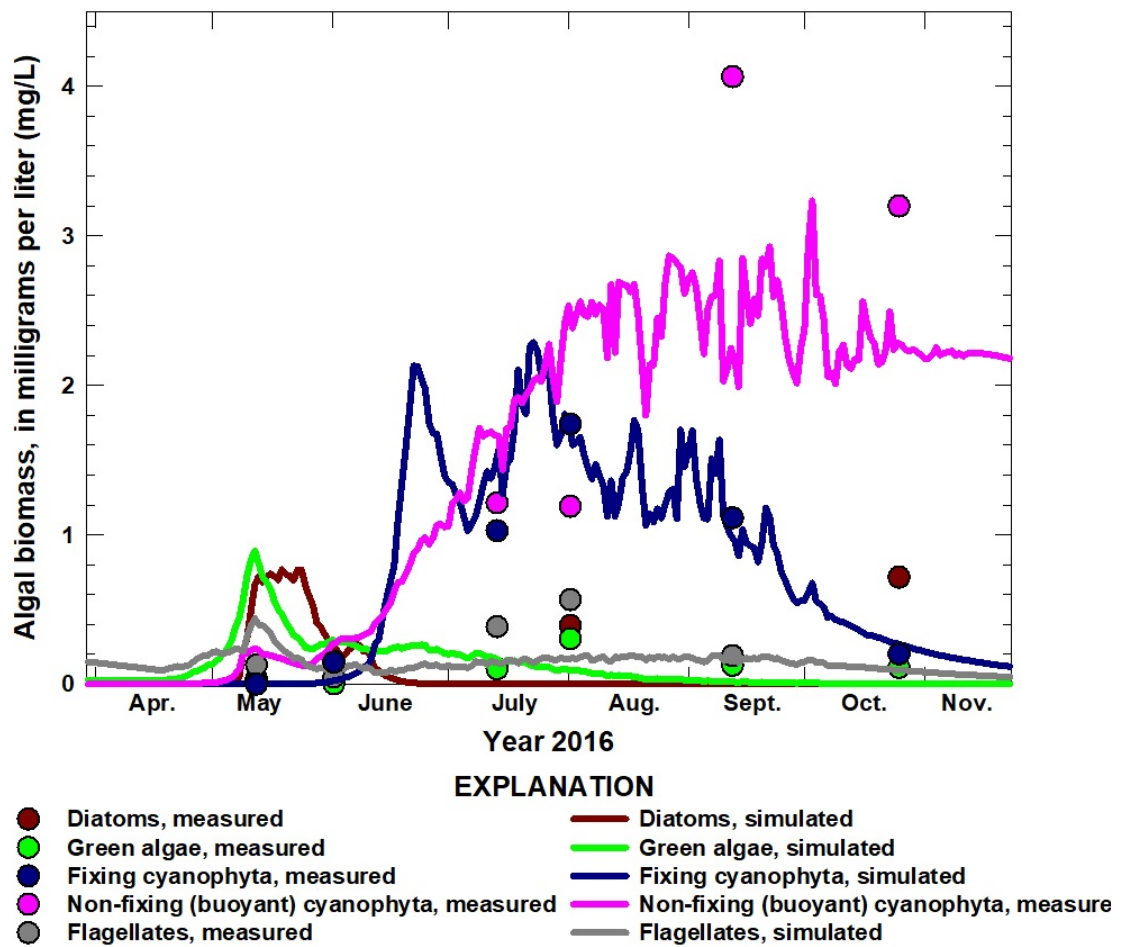


Figure 8: Simulated and measured algal group distributions (diatoms, green algae, fixing cyanophyta, non-fixing (buoyant) cyanophyta, and flagellates) for the 1-meter depth at Madison Lake southwest deep point near Madison Lake, Minn., March 30 to November 23, 2016.

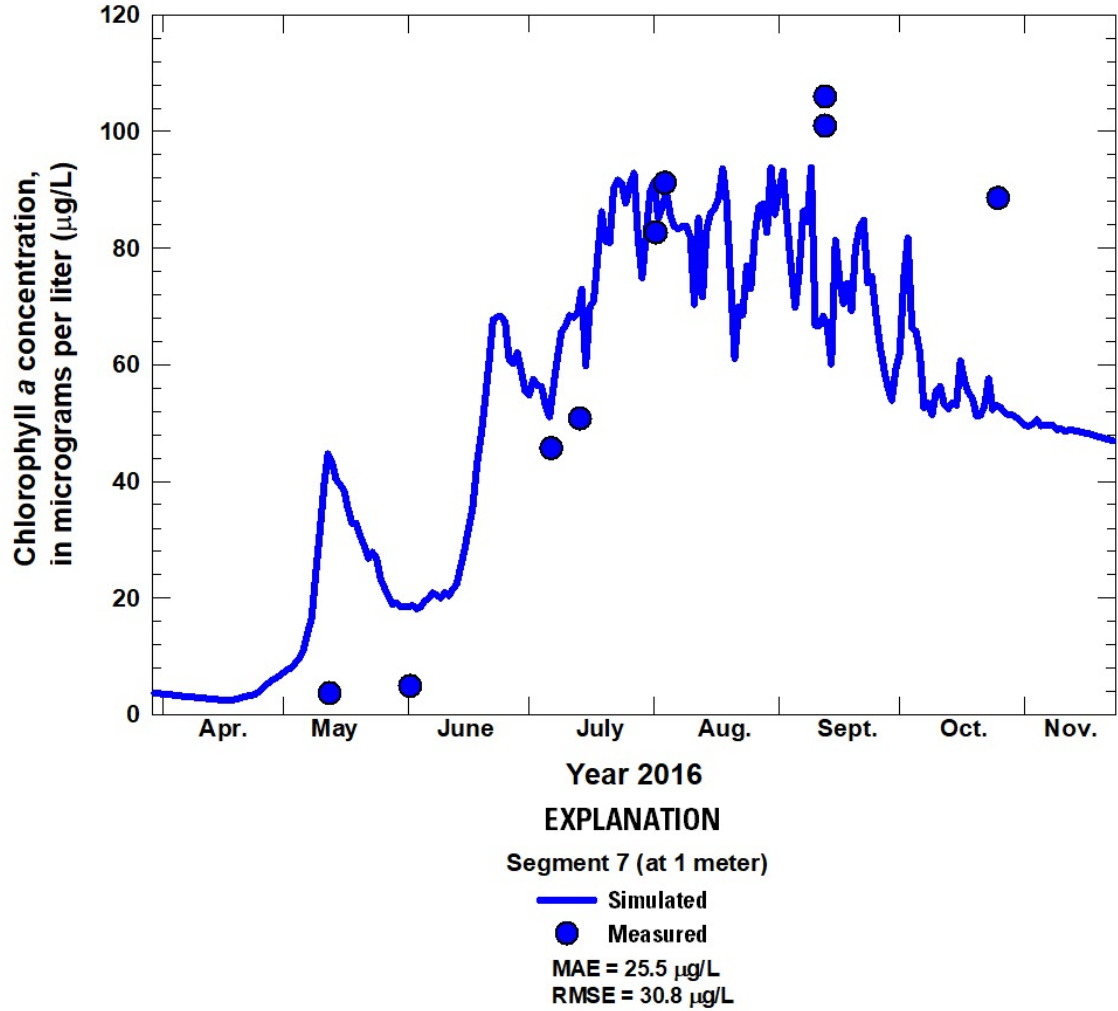


Figure 9: Simulated and measured chlorophyll *a* concentrations for the 1-meter depth at Madison Lake southwest deep point near Madison Lake, Minn. (segment 7) in Madison Lake, March 30 to November 23, 2016.

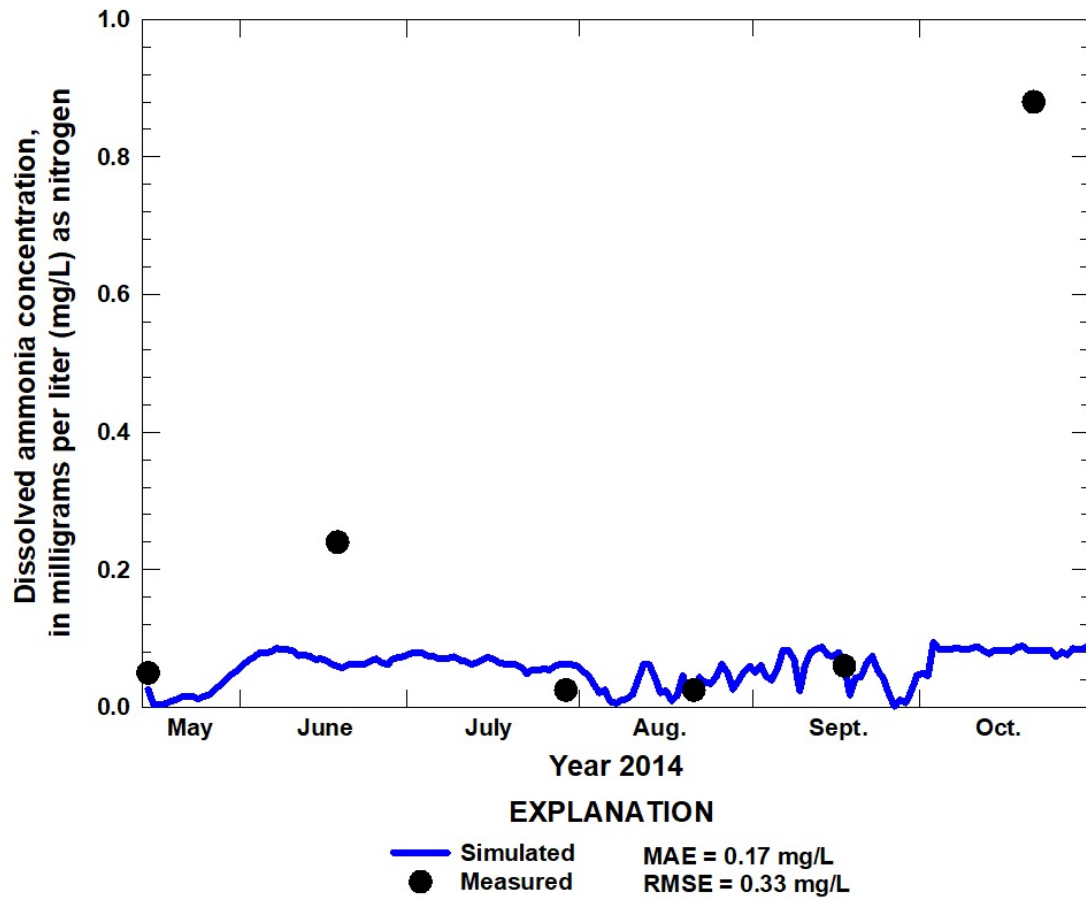


Figure 10: Simulated and measured dissolved ammonia concentrations at 1 meter below the water surface in model segment 7 containing the Madison Lake southwest deep point near Madison Lake, Minn., May 15 to November 1, 2014, with values of mean absolute error (MAE) and root mean square error (RMSE).

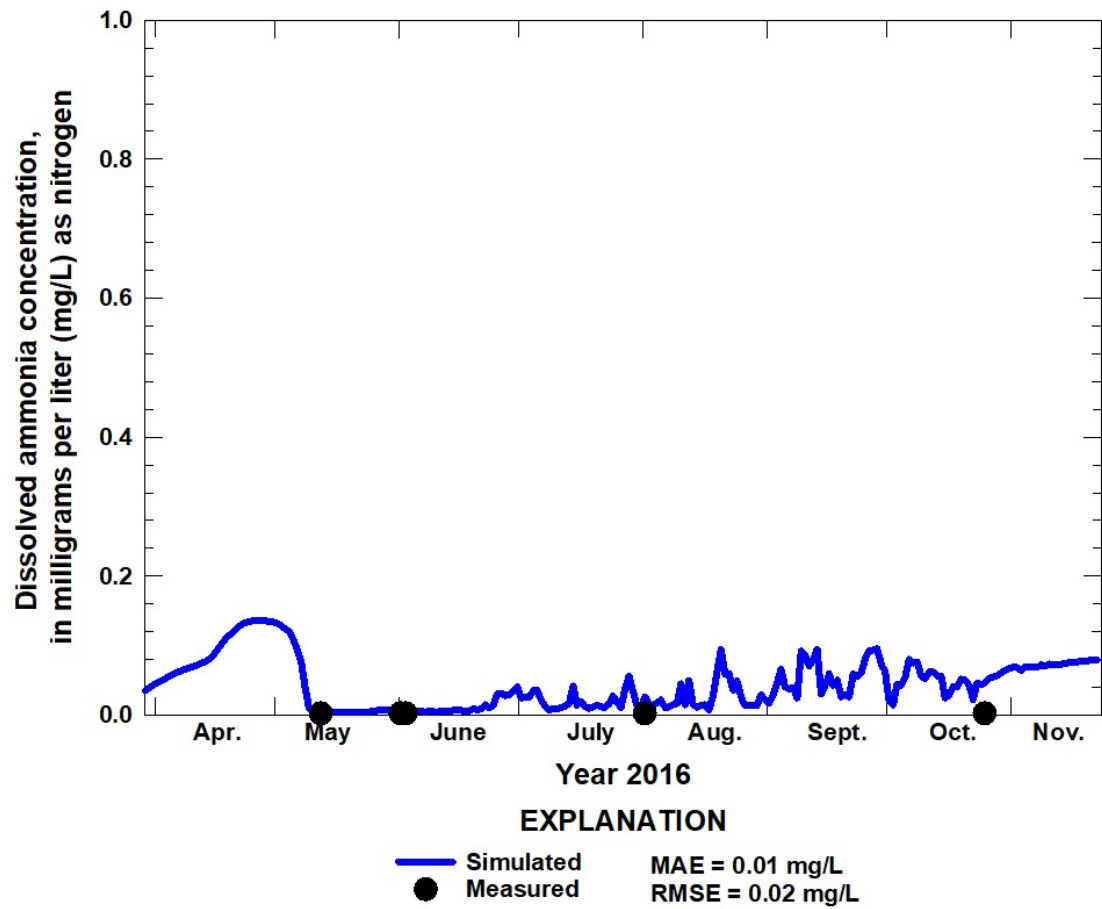


Figure 11: Simulated and measured dissolved ammonia concentrations at 1 meter below the water surface in model segment 7 containing the Madison Lake southwest deep point near Madison Lake, Minn., March 30 to November 23, 2016, with values of mean absolute error (MAE) and root mean square error (RMSE).

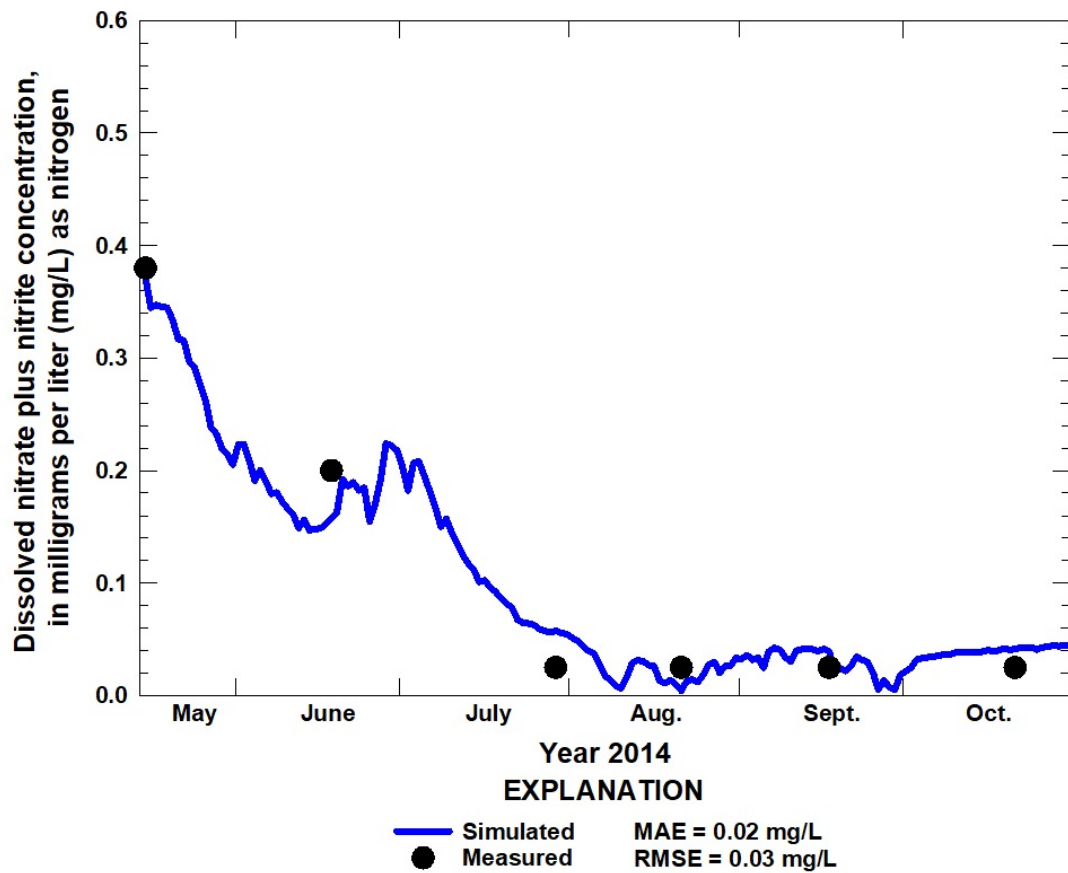


Figure 12: Simulated and measured dissolved nitrate plus nitrite concentrations at 1 meter below the water surface in model segment 7 containing the Madison Lake southwest deep point near Madison Lake, Minn., May 15 to November 1, 2014, with values of mean absolute error (MAE) and root mean square error (RMSE).

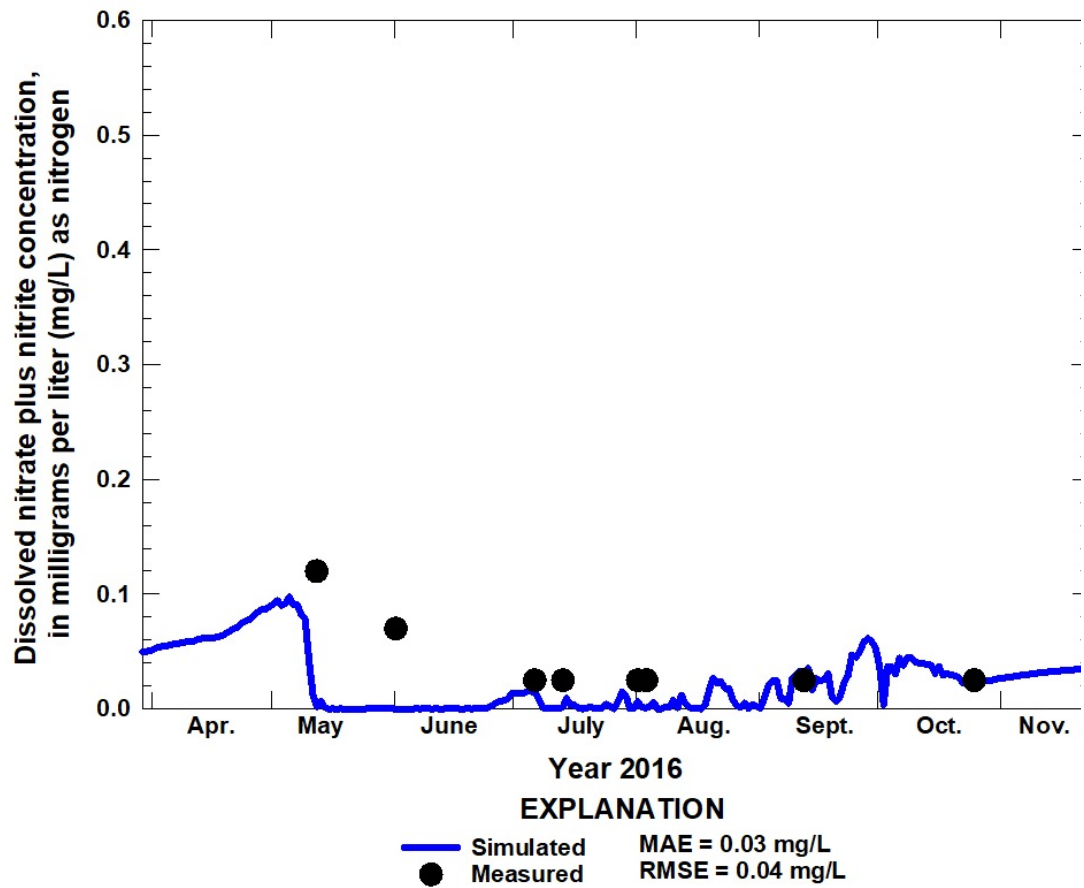


Figure 13: Simulated and measured dissolved nitrate plus nitrite concentrations at 1 meter below the water surface in model segment 7 containing the Madison Lake southwest deep point near Madison Lake, Minn., March 30 to November 23, 2016, with values of mean absolute error (MAE) and root mean square error (RMSE).

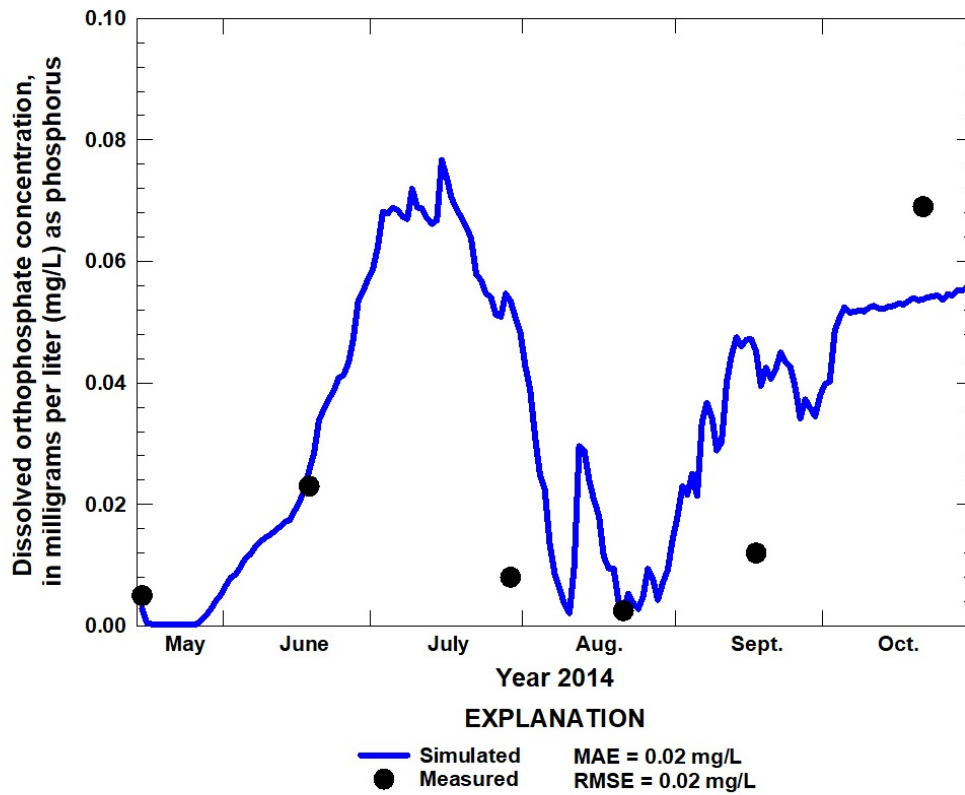


Figure 14: Simulated and measured dissolved orthophosphate concentrations at 1 meter below the water surface in model segment 7 containing the Madison Lake southwest deep point near Madison Lake, Minn., May 15 to November 1, 2014, with values of mean absolute error (MAE) and root mean square error (RMSE).

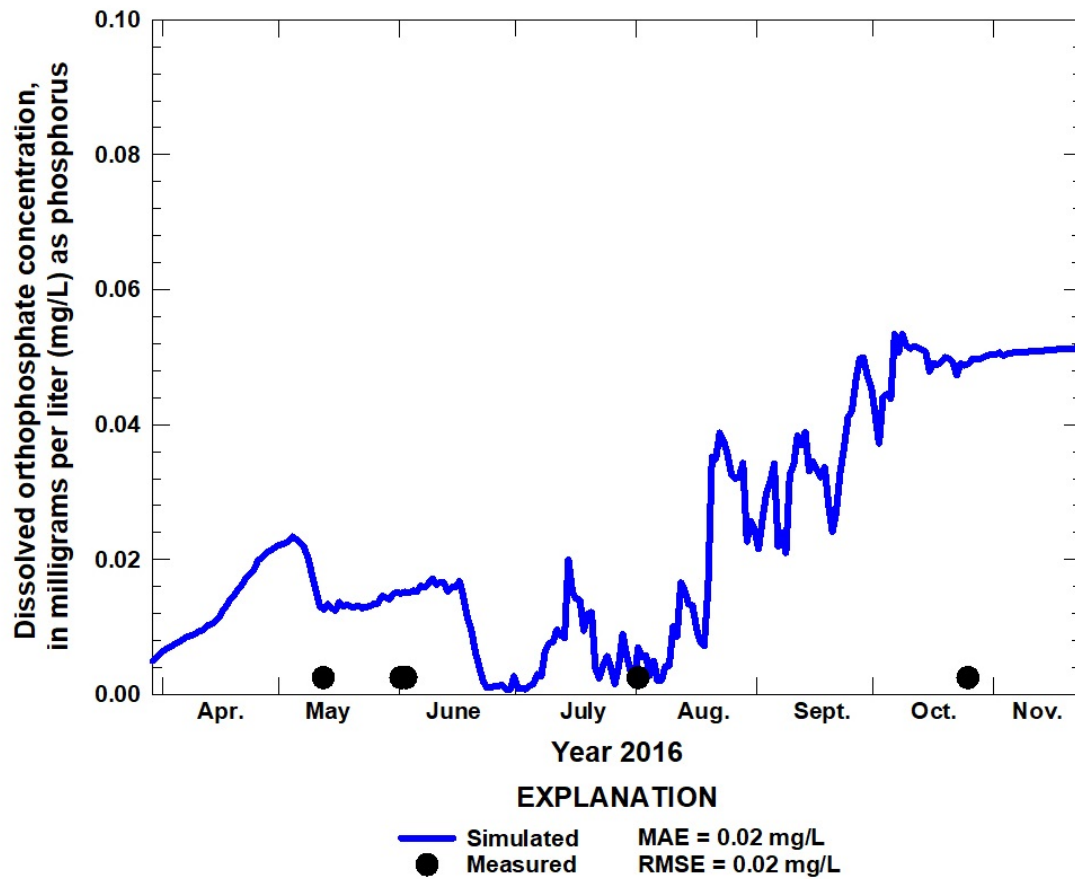


Figure 15: Simulated and measured dissolved orthophosphate concentrations at 1 meter below the water surface in model segment 7 containing the Madison Lake southwest deep point near Madison Lake, Minn., March 30 to November 23, 2016, with values of mean absolute error (MAE) and root mean square error (RMSE).

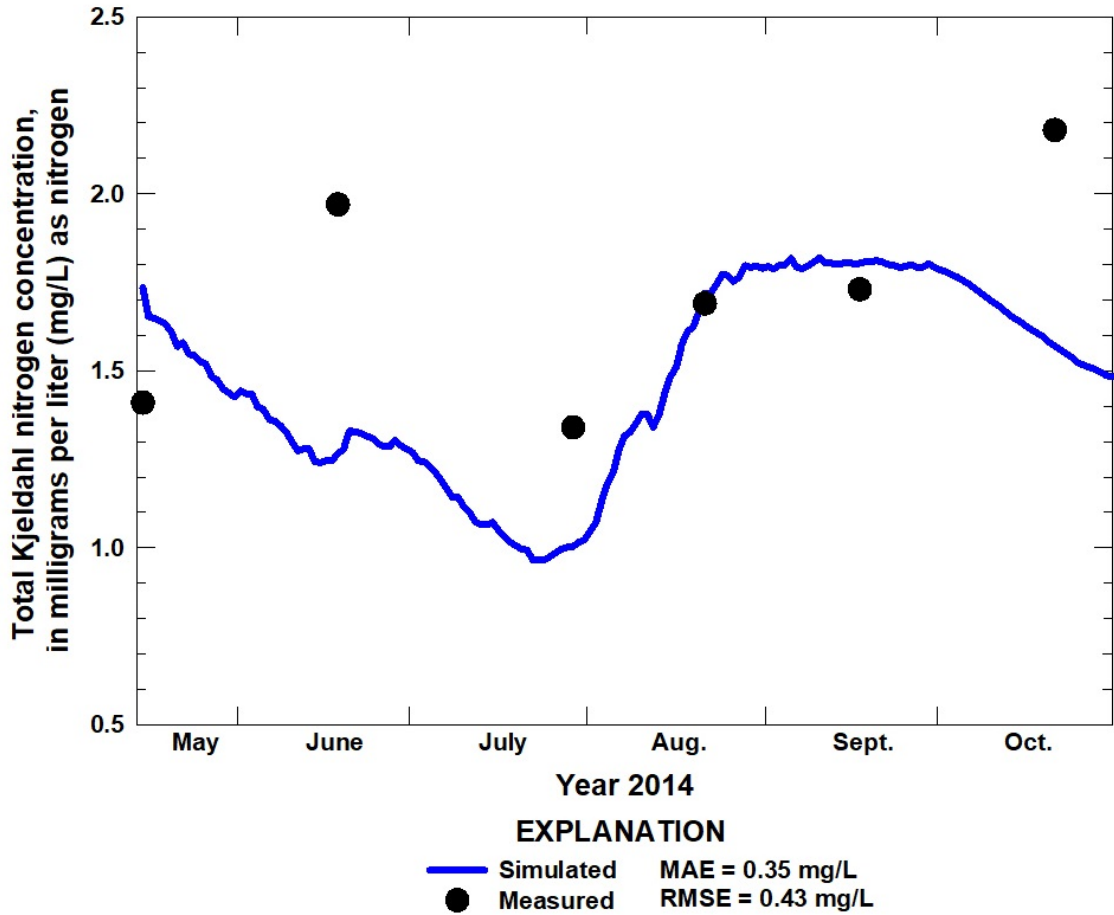


Figure 16: Simulated and measured total Kjeldahl nitrogen concentrations at 1 meter below the water surface in model segment 7 containing the Madison Lake southwest deep point near Madison Lake, Minn., May 15 to November 1, 2014, with values of mean absolute error (MAE) and root mean square error (RMSE).

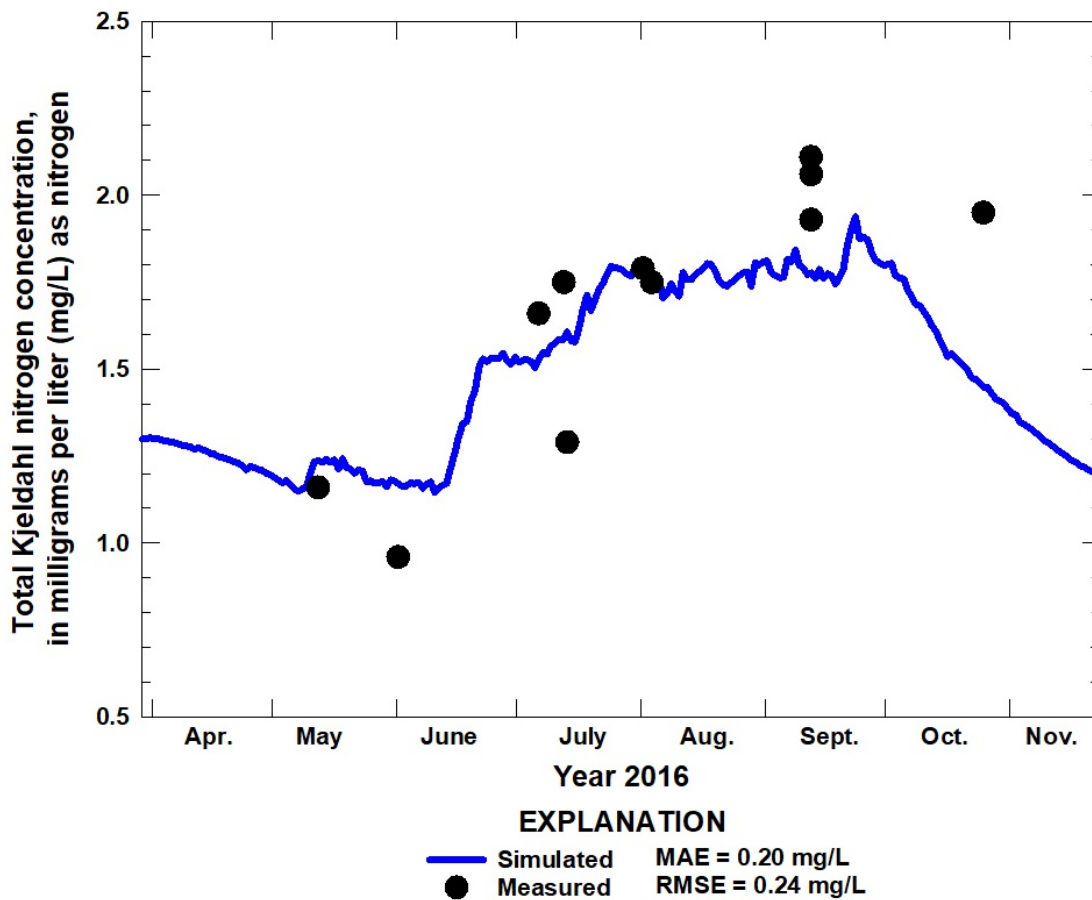


Figure 17: Simulated and measured total Kjeldahl nitrogen concentrations at 2 meters below the water surface in model segment 7 containing the Madison Lake southwest deep point near Madison Lake, Minn., March 30 to November 23, 2016, with values of mean absolute error (MAE) and root mean square error (RMSE).

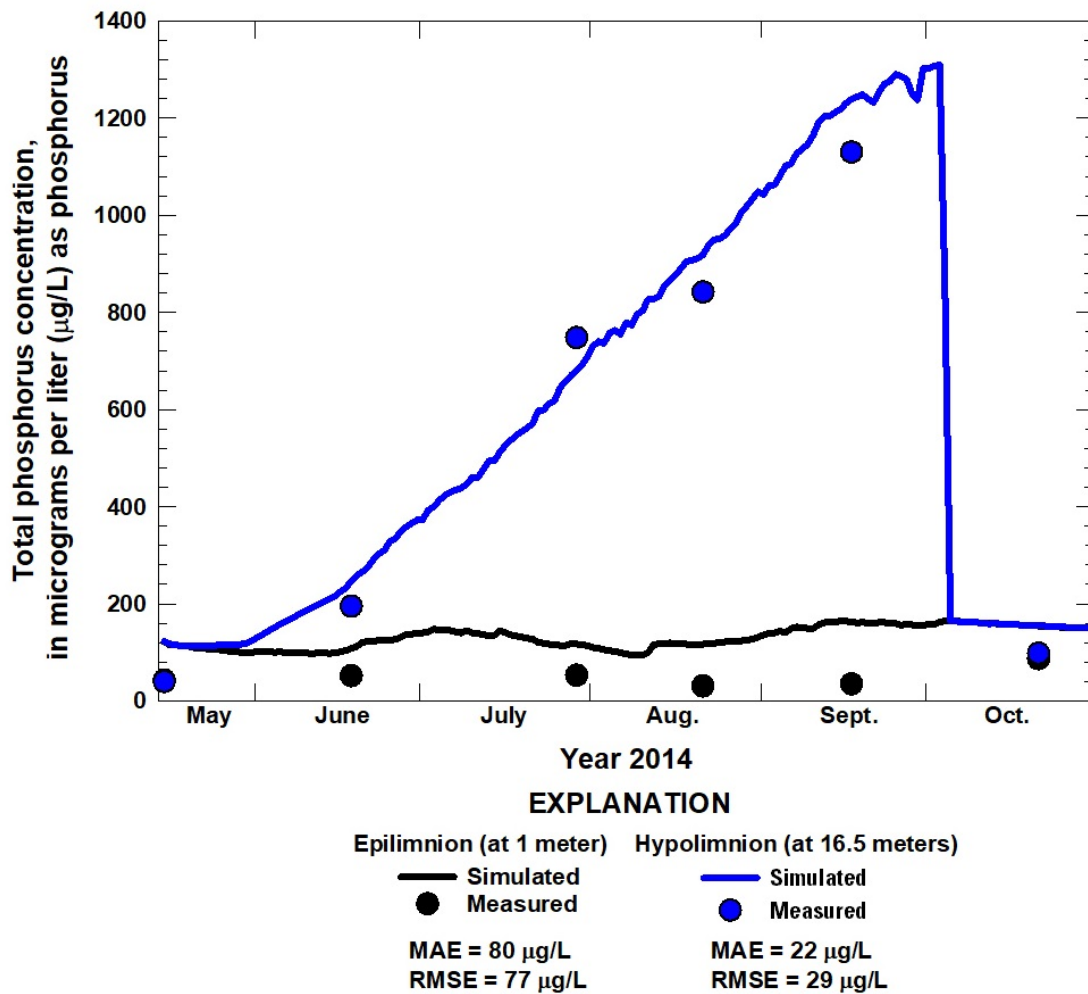


Figure 18: Simulated and measured total phosphorus concentrations at 1 meters and 16.5 meters below the water surface in model segment 7 containing the Madison Lake southwest deep point near Madison Lake, Minn., May 15 to November 1, 2014, with values of mean absolute error (MAE) and root mean square error (RMSE).

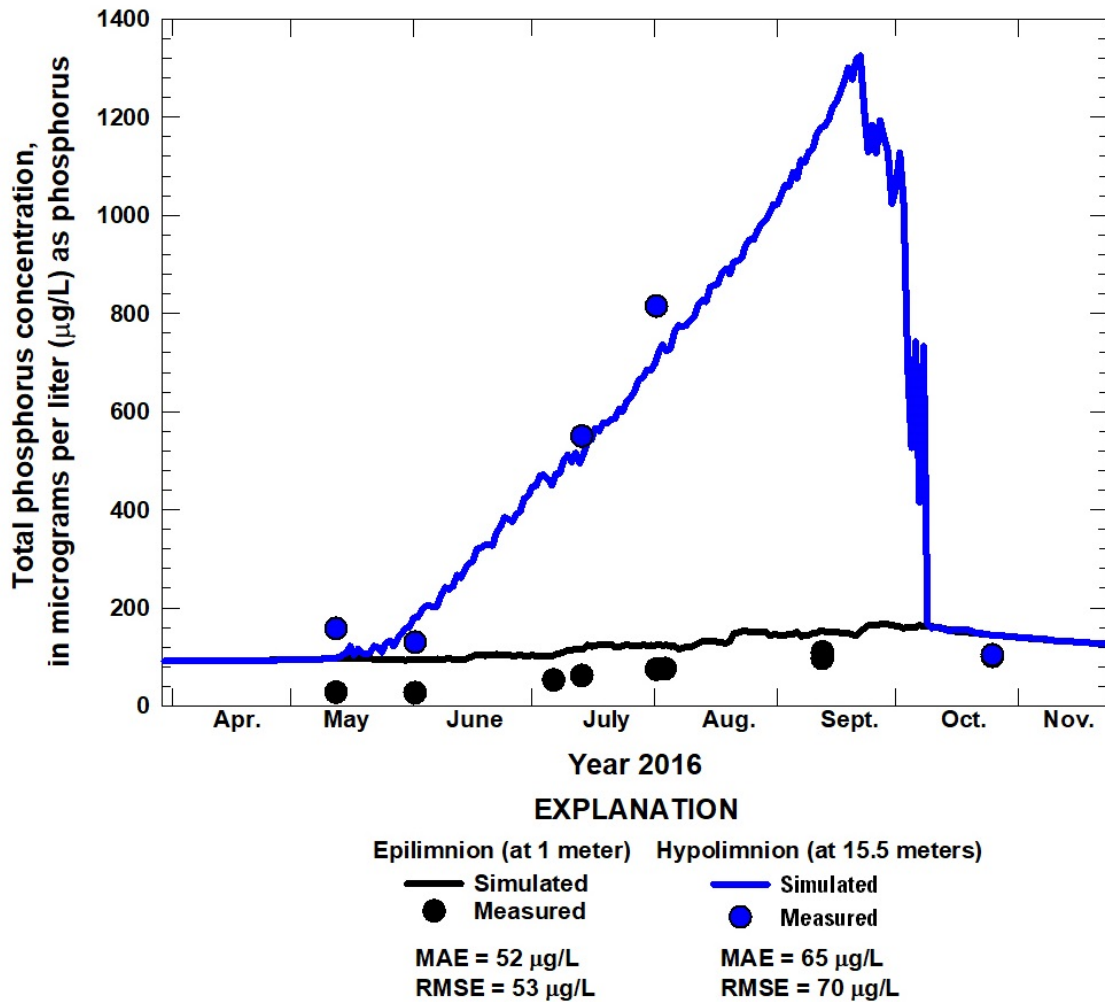


Figure 19: Simulated and measured total phosphorus concentrations at 1 meter and 16.5 meters below the water surface in model segment 7 containing the Madison Lake southwest deep point near Madison Lake, Minn., March 30 to November 23, 2016, with values of mean absolute error (MAE) and root mean square error (RMSE).

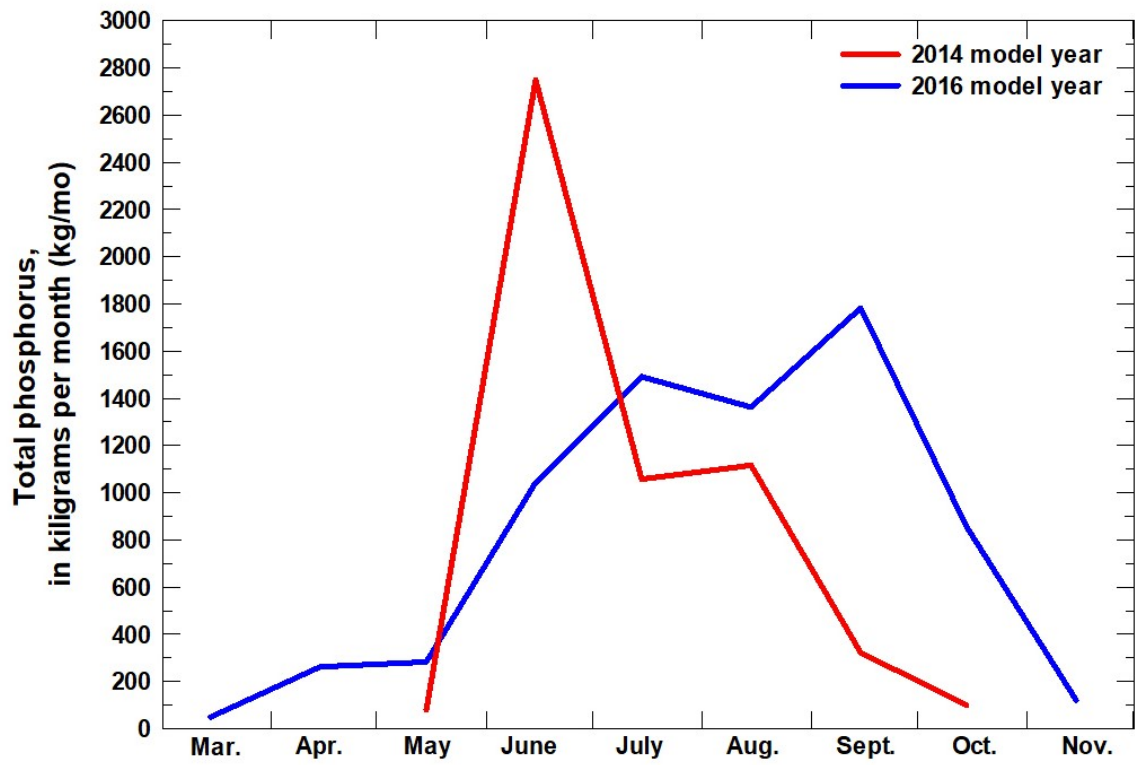


Figure 20: Total phosphorus concentrations monthly, in kilograms per month, for the 2014 and 2016 model years for the updated model.

Table 1. Location of continuous pressure transducers, water-quality sondes, thermistors, and discrete water-quality measurements used for the development of model input or calibration/validation of water temperature, dissolved oxygen, and water-quality constituents.

[All continuous measurements included regular monthly visits to download and calibrate continuous pressure transducers, water-quality sondes, and thermistors. USGS, U.S. Geological Survey; Minn., Minnesota; --, not applicable. Latitude/longitude given in degrees (°), minutes (′), and seconds (″) referenced to the North American Datum of 1983. Continuous constituents: S, water stage level; S→Q, discharge/flow (derived from stage); DO, dissolved oxygen; SC, specific conductance; T, water temperature. Discrete constituents: MI, major inorganics; L-L N, low-level nutrients; TC/TN, total carbon/total nitrogen; Alk, alkalinity; Alg, algae. Use: C, calibration; I, input; WQ, water quality (including discrete constituents). Model segment: number identifies segment inflow/outflow attached to in model; I, inflow; O, outflow]

Site name	Common name in report	USGS station number ¹	Minnesota LakeFinder station number ²	Latitude / longitude	Continuous constituents	Discrete constituents	Use	Model segment
Unnamed stream to Madison Lake at CR-48 near Madison Lake, Minn.	Northeast inlet	05320130	--	44° 11' 53.4"N -93° 46' 39.9"W	S, S→Q, T	DO, pH, SC, T, MI, L-L N, TC/TN, Alk	I	2 (I)
Unnamed stream between Schoolhouse and Goolsby Lakes southeast of Madison Lake, Minn.	Southeast inlet	05320140	--	44° 10' 7.9"N -93° 47' 11.2"W	S, S→Q, T	DO, pH, SC, T, MI, L-L N, TC/TN, Alk	I	12 (I)
Madison Lake outlet to Mud Lake south of Madison Lake, Minn.	Madison Lake outlet	05320170	--	44° 10' 43.7"N -93° 48' 57.1"W	S, S→Q, T	--	S (C), I (S→Q), T (C)	9 (O)
Madison Lake southwest deep point near Madison Lake, Minn.	Southwest deep point	--	07-0044-00-102; 07-0044-00-201	44° 11' 29.8"N -93° 48' 39.7"W	DO, T	DO, pH, SC, T, MI, L-L N, TC/TN, Alk, Alg	WQ (I), T (C), DO (C)	7

¹U.S. Geological Survey, 2016

²Minnesota Department of Natural Resources, 2019b.

Table 2. Water-quality methods for constituents analyzed in water samples from Madison Lake, 2014 and 2016.

[EPA, U.S. Environmental Protection Agency; mg/L, milligrams per meter; SM, standard method; --, not analyzed; µg/L, micrograms per liter; SiO₂, silicon dioxide]

Constituent	Minnesota Department of Health Environmental Laboratory	
	Method	Method detection limit ¹
Dissolved nitrite, as nitrogen	EPA 353.2 (U.S. Environmental Protection Agency, 1993a)	0.01 mg/L
Dissolved nitrite plus nitrate nitrogen	EPA 353.2 (U.S. Environmental Protection Agency, 1993a)	0.05 mg/L
Dissolved ammonia, as nitrogen	EPA 350.1 (U.S. Environmental Protection Agency, 1993b)	0.05 mg/L
Total Kjeldahl nitrogen	EPA 351.2 (U.S. Environmental Protection Agency, 1993c)	0.20 mg/L
Total phosphorus	SM 4500-P (American Water Works Association and others, 1997a)	0.01 mg/L
Dissolved phosphorus	EPA 365.1 (U.S. Environmental Protection Agency, 1993d)	0.01 mg/L
Dissolved orthophosphate	EPA 365.1 (U.S. Environmental Protection Agency, 1993)	0.005 mg/L
Chlorophyll- <i>a</i>	SM 10200-H (American Water Works Association and others, 1997b)	0.001 mg/L
Total dissolved solids	SM 2540C (American Water Works Association and others, 1997c)	10 mg/L
Total silica, as silicon dioxide	SM 4500 SiO ₂ (American Water Works Association and others, 1997d)	0.5 mg/L
Total alkalinity	Inflection point titration (Wilde, 2006)	1 mg/L
Algal counts	ASA (PhycoTech, 2017)	--
Dissolved iron	EPA 200.7 (U.S. Environmental Protection Agency, 2007)	0.001 mg/L

¹The minimum detection limit is the minimum concentration of a substance that can be measured and reported with a 99-percent confidence that the analyte concentration is greater than 0 (U.S. Environmental Protection Agency, 2002).

Table 3. Relative counts and converted algal biomass for (in milligrams per liter) for Madison Lake southwest deep point near Madison Lake, Minnesota, 2014 and 2016.

[mg/L, milligrams per liter]

Algal group or genera	Date	Relative Count	Converted algal biomass (mg/L)
Diatoms (bacillariophyta/crysophyta)	2014-05-14	88	1.584
	2014-06-18	5	0.027
	2014-07-29	38	0.883
	2014-08-21	5	0.185
	2014-09-17	16	0.638
	2014-10-21	1	0.002
	2016-05-12	19	0.035
	2016-06-01	7	0.017
	2016-07-13	4	0.103
	2016-08-01	9	0.392
	2016-09-12	4	0.127
	2016-10-25	32	0.716
	Green algae (chlorophyta)	2014-05-14	6
2014-06-18		9	0.049
2014-07-29		9	0.209
2014-08-21		14	0.517
2014-09-17		6	0.239
2014-10-21		3	0.005
2016-05-12		11	0.020
2016-06-01		1	0.002
2016-07-13		4	0.103
2016-08-01		7	0.305
2016-09-12		4	0.127
2016-10-25		5	0.112
Fixing cyanophyta		2014-05-14	2
	2014-06-18	77	0.417
	2014-07-29	14	0.325
	2014-08-21	57	2.104
	2014-09-17	38	1.516
	2014-10-21	0	0.000
	2016-05-12	0	0.000
	2016-06-01	60	0.148
	2016-07-13	40	1.026
	2016-08-01	40	1.741
2016-09-12	40	1.113	
2016-10-25	9	0.201	

Algal group or genera	Date	Relative Count	Converted algal biomass (mg/L)
Non-fixing (buoyant) cyanophyta	2014-05-14	1	0.018
	2014-06-18	2	0.011
	2014-07-29	31	0.721
	2014-08-21	13	0.480
	2014-09-17	25	0.998
	2014-10-21	1	0.002
	2016-05-12	0	0.000
	2016-06-01	12	0.152
	2016-07-13	36	1.214
	2016-08-01	26	1.190
Flagellates (haptophyta/cryptophyta)	2016-09-12	146	4.064
	2016-10-25	143	3.199
	2014-05-14	3	0.054
	2014-06-18	3	0.016
	2014-07-29	5	0.116
	2014-08-21	8	0.295
	2014-09-17	15	0.599
	2014-10-21	94	0.145
	2016-05-12	70	0.129
	2016-06-01	20	0.049
2016-07-13	15	0.385	
2016-08-01	13	0.566	
2016-09-12	6	0.191	
2016-10-25	9	0.201	

Table 4. Initial constituent concentrations for the Madison Lake CE-QUAL-W2 model: 2014 calibration and 2016 validation runs.

[m NAVD 88; meters above North American Vertical Datum of 1988; mg/L, milligrams per liter; °C, degrees Celsius]

Constituent	Year	
	2014	2016
Initial water-surface elevation, m NAVD 88	310.57	340.38
Total dissolved solids (TDS), mg/L	177.7	272.0
Dissolved orthophosphate, mg/L	0.005	0.005
Dissolved ammonia, as nitrogen, mg/L	0.05	0.035
Dissolved nitrite plus nitrate nitrogen, mg/L	0.38	0.05
Dissolved silica, mg/L	3.95	3.00
Particulate silica, mg/L	1	1
Total iron, mg/L	0.014	0.014
Labile dissolved organic matter (DOM), mg/L	4.9510	3.6759
Refractory DOM, mg/L	11.5522	8.5772
Labile particulate organic matter (POM), mg/L	0.1490	0.2651
Refractory POM, mg/L	0.3478	0.6186
Diatoms/Crysophyta, mg/L	1.4	2.5 x 10 ¹²
Chlorophyta (Green algae), mg/L	5.0 x 10 ⁶	0.0300
Fixing cyanophyta, mg/L	8.0 x 10 ⁶	0.0035
Non-fixing (buoyant) cyanophyta, mg/L	7.5 x 10 ¹³	0.0010
Haptophyta/Cryptophyta, mg/L	1.0 x 10 ⁷	0.1500
Dissolved oxygen, mg/L	0.75-10.25	10
Inorganic carbon, mg/L	170.4	182.2
Alkalinity, mg/L	140.0	149.7
Labile phosphorus partition	0.0065	0.0065
Labile nitrogen partition	0.0950	0.0950
Refractory phosphorus partition	0.0065	0.0065
Refractory nitrogen partition	0.0950	0.0950
Initial temperature, °C	9.9	6.0
Sediment temperature, °C	14.5	12.5
Macrophyte, mg/L	5.0	0.4

^aInitial constituent concentrations were considered uniform throughout the lake for every segment and layer, except in cases with a reported range of values, which constitutes a vertical profile. The highest value is at the surface layer, with the lowest value at the bottom layer, with iterative values in between for each of the layers.

Table 5. Summary of mean absolute error (MAE) and root mean square error (RMSE) values for calibration (2014) and validation (2016) runs for Madison Lake at Madison Lake southwest deep point near Madison Lake, Minnesota (also known as southwest deep point).

[°C, degrees Celsius; Minn. Minnesota; mg/L, milligrams per liter; <, less than; µg/L, micrograms per liter; multiple, integrated vertical profile data]

Constituent	Depth (meters)	Number of compared data points	Calibration Year (2014)		Validation Year (2016)		
			AME	RMSE	AME	RMSE	
Water temperature, °C	multiple	103	0.55	0.70	125	0.67	0.81
Dissolved oxygen, mg/L	multiple	103	0.86	1.22	125	0.91	1.46
Chlorophyll <i>a</i> , µg/L	2	6	22	29	10	26	31
Dissolved orthophosphate, mg/L	2	6	0.02	0.02	5	0.02	0.02
Dissolved ammonia, mg/L	2	6	0.17	0.33	5	0.01	0.02
Dissolved nitrite plus nitrate nitrogen, mg/L	2	6	0.02	0.03	10	0.03	0.04
Total Kjeldahl nitrogen, mg/L	2	6	0.35	0.43	11	0.20	0.24
Total phosphorus, µg/L	2	6	80	77	10	52	53
Total phosphorus, µg/L	16.5	6	22	29	5	65	70
Diatoms (bacillariophyta/crysophyta), mg/L	2	6	0.34	0.46	6	0.36	0.44
Green algae (chlorophyta), mg/L	2	6	0.12	0.13	6	0.28	0.39
Fixing cyanophyta, mg/L	2	6	0.45	0.50	6	0.13	0.19
Non-fixing (buoyant) cyanophyta, mg/L	2	6	0.74	1.03	6	0.81	1.02
Flagellates (haptophyta/cryptophyta), mg/L	2	6	0.13	0.17	6	0.19	0.23

Table 6. Summary of phosphorus loading for updated Madison Lake model (2014, 2016), original Madison Lake model, and two phosphorus loading scenarios, according to load estimates and internal CE-QUAL-W2 calculations. Negative terms denote a loss term due to the net export of phosphorus (from the distributary tributary flow).

Model Year/Scenario	Scenario Number	Component	March	April	May	June	July	Aug.	Sept.	Oct.	Nov.	Total
			kilograms/month									
Model run, March 29-November 23, 2016	1	Organic Matter	28.82	141.2	123.1	180.1	285.0	274.6	746.4	412.2	64.27	2256
		Orthophosphate, external load	20.52	100.6	92.40	177.3	338.6	287.1	727.2	385.5	42.69	2172
		Orthophosphate, internal load	0.651	21.18	67.79	686.1	868.8	801.6	309.4	58.25	15.05	2829
		Total Phosphorus	49.99	262.9	283.3	1044	1492	1363	1783	855.9	122.0	7256
		Internal load, percentage of total phosphorus	1.3%	8.1%	23.9%	65.7%	58.2%	58.8%	17.4%	6.8%	12.3%	39.0%
Model run (updated model), May 15-November 1, 2014	2	Organic Matter	--	--	-46.81	909.3	187.0	98.36	18.30	23.80	--	1190
		Orthophosphate, external load	--	--	81.17	1252	258.6	75.54	13.17	16.32	--	1697
		Orthophosphate, internal load	--	--	45.71	588.0	612.6	942.6	291.2	58.92	--	2539
		Total Phosphorus	--	--	80.06	2750	1058	1116	322.7	99.04	--	5426
		Internal load, percentage of total phosphorus	--	--	57.1%	21.4%	57.9%	84.4%	90.2%	59.5%	--	46.8%
Model run (original model), May 15-November 1, 2014	3	Organic Matter	--	--	-46.81	909.3	187.0	98.36	18.30	23.80	--	1190
		Orthophosphate, external load	--	--	81.17	1252	258.6	75.54	13.17	16.32	--	1697
		Orthophosphate, internal load	--	--	41.01	479.8	628.0	951.0	204.0	53.77	--	2358
		Total Phosphorus	--	--	75.37	2641	1074	1125	235.5	93.89	--	5244
		Internal load, percentage of total phosphorus	--	--	54.4%	18.2%	58.5%	84.5%	86.6%	57.3%	--	45.0%

Model Year/Scenario	Scenario Number	Component	March	April	May	June	July	Aug.	Sept.	Oct.	Nov.	Total
			kilograms/month									
Model run (original model), May 15-November 1, 2014, increasing external orthophosphorus load (20 percent)	4	Organic Matter	--	--	-46.81	909.3	187.0	98.36	18.30	23.80	--	1190
		Orthophosphate, external load	--	--	97.78	1503	310.3	90.52	15.76	19.56	--	2037
		Orthophosphate, internal load	--	--	40.73	480.9	628.8	956.5	208.7	53.73	--	2369
		Total Phosphorus	--	--	91.69	2893	1126	1145	242.8	97.08	--	5596
		Internal load, percentage of total phosphorus	--	--	44.4%	16.6%	55.8%	83.5%	86.0%	55.3%	--	42.3%
Model run (original model), May 15-November 1, 2014, decreasing external orthophosphorus load (20 percent)	5	Organic Matter	--	--	-46.81	909.3	187.0	98.36	18.30	23.80	--	1190
		Orthophosphate, external load	--	--	64.46	1001	206.8	60.38	10.48	12.96	--	1356
		Orthophosphate, internal load	--	--	41.31	480.5	630.7	949.3	202.0	54.05	--	2358
		Total Phosphorus	--	--	58.95	2391	1025	1108	230.7	90.81	--	4904
		Internal load, percentage of total phosphorus	--	--	70.1%	20.1%	61.6%	85.7%	87.5%	59.5%	--	48.1%

